



Review:

A review on the developments and space applications of mid- and long-wavelength infrared detection technologies*

Yuying WANG^{†1}, Jindong LI^{†‡2}, Hezhi SUN², Xiang LI²

¹Beijing Institute of Spacecraft System Engineering, China Academy of Space Technology, Beijing 100094, China

²Institute of Remote Sensing Satellite, China Academy of Space Technology, Beijing 100094, China

[†]E-mail: y-y.wang@outlook.com; ljdcast@163.com

Received Mar. 29, 2023; Revision accepted Nov. 29, 2023; Crosschecked June 5, 2024

Abstract: Mid-wavelength infrared (MWIR) detection and long-wavelength infrared (LWIR) detection constitute the key technologies for space-based Earth observation and astronomical detection. The advanced ability of infrared (IR) detection technology to penetrate the atmosphere and identify the camouflaged targets makes it excellent for space-based remote sensing. Thus, such detectors play an essential role in detecting and tracking low-temperature and far-distance moving targets. However, due to the diverse scenarios in which space-based IR detection systems are built, the key parameters of IR technologies are subject to unique demands. We review the developments and features of MWIR and LWIR detectors with a particular focus on their applications in space-based detection. We conduct a comprehensive analysis of key performance indicators for IR detection systems, including the ground sampling distance (GSD), operation range, and noise equivalent temperature difference (NETD) among others, and their interconnections with IR detector parameters. Additionally, the influences of pixel distance, focal plane array size, and operation temperature of space-based IR remote sensing are evaluated. The development requirements and technical challenges of MWIR and LWIR detection systems are also identified to achieve high-quality space-based observation platforms.

Key words: Infrared detection; Space application; Mid- and long-wavelength infrared detection; Space-based Earth observation; Remote sensing

<https://doi.org/10.1631/FITEE.2300218>

CLC number: TP73; V45

1 Introduction

By leveraging the advantages of space platforms such as wide coverage, global observation, and reduced interference, infrared (IR) detection systems play an important role in Earth observation and universe exploration. Space-based IR Earth observation offers diverse applications, including marine observation, meteorology, surveying and mapping, agriculture, forestry, environment monitoring, disaster detection, and

national defense (Saraf et al., 2008; Gao et al., 2016; Sobrino et al., 2016; Khanal et al., 2017; Karthikeyan et al., 2020; Yang CH, 2020; Li JD, 2021). It offers strong anti-interference capabilities and the ability to identify disguised targets effectively (Karim and Andersson, 2013; Bhan and Dhar, 2019). Furthermore, space-based IR detection holds particular significance for missile early warning and military reconnaissance, prompting its development by countries such as the US, Russia, and France (Watson and Zondervan, 2008; Zheng et al., 2008; Bhan and Dhar, 2019). The Defense Support Program (DSP), Space-Based Infrared System (SBIRS), Mid-Course Space Experiment (MSX), Near-Field Infrared Experiment (NFIRE), Space Tracking and Surveillance System (STSS), and the Next-Generation Overhead Persistent Infrared

[‡] Corresponding author

* Project supported by the National Basic Research Program of China (No. 613322), the Beijing Nova Program, China (No. Z211100002121078), and the National Natural Science Foundation of China (No. 52202506)

ORCID: Yuying WANG, <https://orcid.org/0000-0002-3071-1386>; Jindong LI, <https://orcid.org/0009-0006-5774-212X>

© Zhejiang University Press 2024

(NG-OPIR) are some of the world-renowned satellite systems developed by the US for defense purposes (Bartschi et al., 1996; Paxton et al., 1996; Price et al., 1998). To enable the rapid identification and tracking of mid-course missiles and hypersonic aircrafts in the future, mid-wavelength IR (MWIR) and long-wavelength IR (LWIR) detectors with high detectivity and sensitivity are among the leading technologies requiring development (Robbins, 2019). Additionally, the detection capabilities of LWIR and far IR (FIR) are indispensable for observing far, faint, and cold objects in the cosmos, including planets, stars, and galaxies, and for investigating the origins of the universe (Sanders, 2004; Schwalm et al., 2005; Hirabayashi et al., 2008; Nakagawa et al., 2012; Bhan and Dhar, 2019; Park S et al., 2019; Rogalski, 2019; Ma et al., 2023). The US, Japan, and Europe have launched several astronomical exploration telescopes equipped with IR detection devices, including the latest ones, James Webb Space Telescope (JWST) and Space Infrared Telescope for Cosmology and Astrophysics (SPICA) (Ishihara et al., 2003; Ressler et al., 2008; Onaka et al., 2010; Nakagawa et al., 2012; Laureijs et al., 2014; Rieke et al., 2015; Wright et al., 2015). However, as astronomical observations extend to increasingly remote celestial objects, both the target signals and background radiation become exceedingly faint, thereby imposing more stringent demands on the fabrication of IR detectors. These demands encompass the need for higher resolution, heightened sensitivity, enhanced detectivity, and the production of large-format focal plane arrays (FPAs) (Rieke, 2007; Farrah et al., 2019).

IR detectors have evolved from unit detectors, line arrays, single-color FPAs, and double-color FPAs to the current multi-color FPA (Martyniuk et al., 2014). Currently, the detector array formats of Raytheon Vision Systems (RVS) have transitioned from 1 k×1 k to 8 k×8 k (Starr et al., 2016) to multi-color and hyperspectral detection, while the detection band has expanded to a very-long-wavelength band. To meet the increasing demands for high-performance IR detectors for space IR detection systems (Rogalski, 2002, 2005; Nakagawa et al., 2012; Long MS et al., 2019), researchers have been developing and improving high-performance cryogenic MWIR and LWIR detectors, such as HgCdTe, Si:As, and type-II superlattice (T2SL). Notably, HgCdTe and Si:As FPAs can perform

with low dark current, small noise, and high detectivity under a cryogenic environment and have been widely applied in space-based Earth observation and astronomical exploration. However, HgCdTe FPA detectors face significant manufacturing difficulties in a large format and at a long wavelength (Lyu et al., 2022). Although T2SL detectors are considered the most promising alternative to large format HgCdTe detectors for MWIR and LWIR, they have low quantum efficiency and immature development, and have not yet been used in space applications (Alshahrani et al., 2022). Quantum well infrared photodetectors (QWIPs) have been tested in space and applied in Landsat 8/9 satellites, which were launched by the US (Hickey et al., 2018; Jhabvala et al., 2020), but they have not been extensively used.

Reducing the operation temperature is an important approach to reducing the dark current noise and the background scatter radiation noise and improving the sensitivity, detectivity, and operation range of IR detectors (Blazejewski et al., 1994; Kinch, 2000; Rogalski, 2003b). Consequently, the leading space observation systems for Earth observation, military reconnaissance, meteorology, and astronomy, developed by the US, Japan, Europe, and China, have established cryogenic optical systems (Abbott et al., 2000; Rogalski, 2002; Roberts and Roush, 2007; Martyniuk et al., 2014; Starr et al., 2016; Long MS et al., 2019; Wu YN et al., 2019; Jiang et al., 2021). The operation temperature of these high-performance detectors ranges from the ultra-cryogenic temperature of about 100 mK to a cryogenic temperature of about 80 K. However, maintaining a low-temperature operating environment to ensure the performance of IR detectors poses challenges for the miniaturization, longevity, and cost-effective applications of the system.

Since the concept of developing small-size, lightweight, low-energy-consumption, low-price, and high-performance (SWaP³) IR detectors was proposed in 2010 (Ge et al., 2022; Guo JX et al., 2022), the leading trend of next-generation IR detectors has evolved towards incorporating large format size, miniaturization, double-color/multi-color capabilities, and enhanced intelligence. To reduce high cost caused by cryogenic systems, researchers have been developing high operation temperature (HOT) IR detectors that can work up to 150 K, such as p-on-n HgCdTe, P⁻-v-N⁺ HgCdTe,

XBn barrier blocking InAsSb, and InAs/InAsSb (Qin et al., 2021; Zhang KJ, 2021; Chen ZC et al., 2022; Hao et al., 2022; Song et al., 2022; Chen J et al., 2023; Ting et al., 2023). There are also several new types of IR detectors that aim to operate at room temperature, including plasma-enhanced IR detectors (PEIDs), quantum cascade IR detectors based on energy band engineering (QCIDs-EBE), interband cascade detectors (ICDs), and low-dimensional material IR detectors. Additionally, some detectors have been developed to enhance the response in a wider band; one such example is the photon-trapping structure IR detector based on artificial photon microstructure control (IRAPMC). However, the detectivity and overall performance of such detectors still need to be improved and their fabrication challenges need to be addressed (Gendron et al., 2004; Giorgetta et al., 2009; Rogalski, 2011; Hu et al., 2019). The development of cutting-edge manufacturing technologies, such as artificial microstructure and artificial intelligence, is expected to lead to innovations in the fabrication of IR detectors, as well as on-chip intelligence and chip-level integration.

In the literature, a multitude of reviews have focused on the development of existing IR detector technologies (Sclar, 1984; Rogalski, 2003a, 2008, 2009, 2010, 2011, 2012, 2017, 2019; Martyniuk et al., 2014; Rogalski et al., 2016, 2019a, 2019b, 2020; Bhan and Dhar, 2019; Ye et al., 2022). However, as the demands for advanced and efficient space-based remote sensing systems continue to grow, the requirements for IR detection systems have evolved towards higher spatial resolution, greater temporal resolution, enhanced spectral resolution, and improved radiometric resolution. This presents new challenges for MWIR and LWIR detectors due to the requirements of larger format size, increased detectivity, higher level of integration, and smaller pixel size. Thus, it is crucial to provide a more comprehensive exposition of the applications, developments, requirements, and challenges of IR detection technologies. We specifically focus on the development of MWIR and LWIR detectors and their applications in space-based remote sensing, Earth observation, and astronomical observation. Furthermore, in light of the forthcoming demands of space-based observations, the technical challenges and development trends of MWIR and LWIR detectors are analyzed and summarized.

2 Development of IR detectors

2.1 Basics of IR detection

Any object with a temperature above absolute zero (0 K) radiates electromagnetic waves. According to Planck's law, the thermal emission of an ideal black body is a function of wavelength and temperature. For general objects, the emission at a given wavelength is determined by their surface temperature as well as their thermal physical properties (Bergman et al., 2011). As indicated in Wien's displacement law (Eq. (1)) (Bergman et al., 2011; Rogalski, 2011), the wavelength with the maximum electromagnetic radiation intensity of an object is inversely proportional to its temperature. In essence, the radiation spectrum of objects with a lower temperature is centered in a longer spectral band, and vice versa (Fig. 1).

$$\lambda_{\max} T_{\text{obj}} = 2898 \mu\text{m} \cdot \text{K}. \quad (1)$$

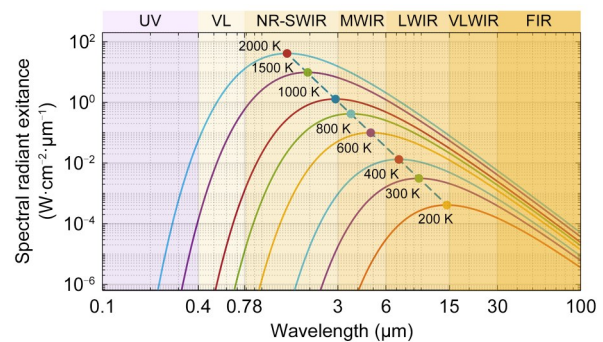


Fig. 1 Relationship between wavelength and spectral radiant exitance based on Planck's law

According to the literature, there are several different sub-division schemes of the IR spectrum (Miller, 1994, 2004). A commonly used definition is provided as follows: the near-IR (NIR) spectral region ranges from 0.75 to 1.4 μm ; the short-wavelength IR (SWIR) region ranges from 1.4 to 3.0 μm ; the MWIR region ranges from 3 to 8 μm ; the IR LWIR region ranges from 8 to 15 μm ; the very-long-wavelength IR (VLWIR) region ranges from 15 to 30 μm ; the FIR region extends from 15 to 1000 μm , according to the encyclopedia of laser physics and technology (Paschotta, 2008). In the context of remote sensing applications, the MWIR band of 3–5 μm and the LWIR band of 8–14 μm are mainly used.

2.2 Types and features of MWIR and LWIR detectors

Electromagnetic waves can be detected and transformed into visible image signals by sensors to identify, position, and track targets. IR detectors are specifically used to sense the electromagnetic wave emitted by the target in the IR range, and semi-conductive photon detectors serve predominantly in IR detection systems (Tidrow and Dyer, 2001; Wu BH et al., 2002; Huang et al., 2018; Teng et al., 2019). When IR photons with different energies are absorbed by the semiconductor material of an IR detector, electron-cavity pairs are excited inside it, thus changing the carrier distribution. As the carriers are collected by the electrode under an electric field, the photo-generated voltage signal variation would reflect the energy distribution of the detected target (Rogalski et al., 2009). The closer the response wavelength of the IR detector is to the peak radiation wavelength of the target, the stronger the detector response will be (Fig. 2). If the target radiant wavelength exceeds the cut-off wavelength of the detector, no significant response will be produced. According to Wien's displacement law and Planck's law, the detection of lower-temperature targets, characterized by longer peak radiation wavelengths, necessitates the use of IR detectors with longer cut-off wavelengths being needed.

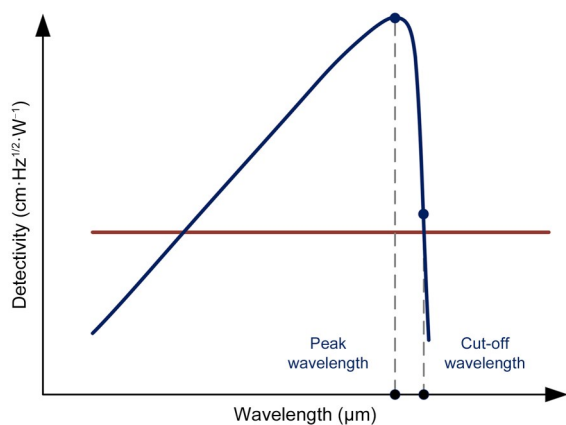


Fig. 2 Relative spectral response for photon and thermal detector (constant incident radiant power) (Rogalski, 2019)

The material of popular MWIR and LWIR detectors has several types, including HgCdTe (Kinch, 2000; Rogalski, 2003a), InSb, InAs/GaSb T2SL (Rogalski, 2003a), GaAs/AlGaAs quantum well (QW), quantum

dot (QD), arsenic-doped silicon-blocked impurity band (Si:As BIB), VO_x, a-Si, and superconductor (Kruse, 2001; Hoffman et al., 2004; Schneider and Liu, 2007; Gunapala et al., 2011; Rogalski, 2011; Migdall et al., 2013; Rogalski et al., 2017; Liu JK et al., 2019). The response wavelength of some IR detector materials is displayed in Fig. 3. Additionally, studies have indicated that a cut-off wavelength of 30 μm has been achieved for HgCdTe and QWIP materials, 32 μm for T2SL material (Wei et al., 2002), and 19 μm for HgCdTe FPA (Gravrand et al., 2017).

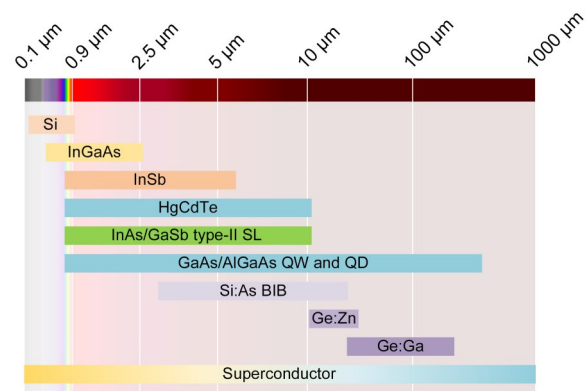


Fig. 3 Potential materials working at different infrared wavelengths

2.3 Classification of IR detectors by operation temperature

IR detectors can be classified into two categories according to their different operation temperatures: cooled and uncooled. Cooled IR detectors refer to detectors that require cooling mechanisms, such as cooling with cryogenic coolers, to maintain a very low operation temperature to enhance their sensitivity and reduce noise levels (Bhan and Dhar, 2019). Cryogenic cooling enables the detectors to detect faint IR signals and achieve higher image resolution, sensitivity, detectivity, responsiveness, and detection range. Therefore, cooled IR detectors are typically used in space detection and military night vision. On the other hand, uncooled IR detectors use materials or technologies that can be functional without the need for extreme cooling, and can operate at temperatures close to room temperature. Uncooled detectors are often more power-efficient and cost-effective compared to cooled ones. However, their detectivity, sensitivity, and responsiveness may be relatively low, and they are

more susceptible to noise and thermal variations. As a result, uncooled IR detectors are used mainly in civilian areas where high-volume application requirements take priority over imaging quality.

At higher operation temperatures, the background radiation noise caused by stray light can seriously affect the imaging quality of long-wave IR detectors. Thus, for the best detectivity, MWIR and LWIR detectors should operate at cryogenic temperatures (Fig. 4) (Piotrowski and Gawron, 1997; Rogalski, 2019). In astronomy- and space-based early warning, IR detectors with higher detectivity and lower operation temperatures are necessary for obtaining a significant response to the distant and faint targets. For example, charge-sensitive infrared photo-transistor (CSIP) and QD detectors can achieve a detectivity of $10^{15} \text{ cm}\cdot\text{Hz}^{1/2}\cdot\text{W}^{-1}$ (at 4.2 K) and $10^{18} \text{ cm}\cdot\text{Hz}^{1/2}\cdot\text{W}^{-1}$ (at 100 mK) under ultralow temperatures (Fig. 4) (Rogalski, 2019).

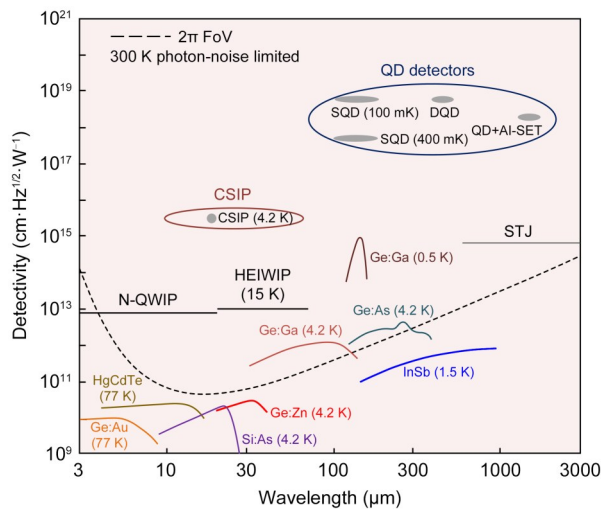


Fig. 4 Detectivity of various infrared detectors (Rogalski, 2019)

2.4 Developments of high-performance MWIR and LWIR detectors

2.4.1 Evolution and role of IR detectors in space remote sensing

IR detectors have evolved from unit detectors, line arrays, single-color FPAs, and double-color FPAs to the current 4th generation, which features multi-color FPAs (Fig. 5) (Tidrow and Dyer, 2001; Rogalski, 2019; Rogalski et al., 2020; Zhang S et al., 2020;

Chang et al., 2021; Pan et al., 2023). From the advent of the 2nd generation FPA IR onwards, the number of pixels has significantly increased, which also enabled staring imaging. The forthcoming evolution of the 4th generation IR detectors will emphasize heightened sensitivity, improved resolution, very long wavelength, and multi-color capabilities (Tidrow and Dyer, 2001; Wu BH et al., 2002; Rogalski, 2009, 2017, 2019; Rogalski et al., 2016, 2019a, 2019b, 2020; Bhan and Dhar, 2019; Zhang S et al., 2020; Chang et al., 2021; Pan et al., 2023). In recent years, progress in this field has been accelerated by on-chip intelligence and chip-level integration technologies, along with the growth of artificial microstructure and artificial intelligence (Ye et al., 2022; Zhu et al., 2022).

Taking advantage of imaging in different bands, the detection sensitivity of double-color/multi-color detectors has been increased, and the photoelectric confrontation abilities of anti-decoy and anti-stealth characteristics have thus been improved, which reduces the probability of misidentifying targets and minimizes false alarms (Sweeney et al., 2020). High-performance IR detectors have been widely applied in the aerospace remote sensing and weaponry fields in Europe and the US since the end of the 20th century. Line array and unit IR detectors can be used in space applications for imaging by way of push-broom scanning, swing scanning, and circular scanning methods. They have a large imaging swath and can be applied for reconnaissance purposes. While FPA IR detectors can use only push-broom scanning for imaging in space applications, they have a narrower imaging swath compared to scan-to-image detectors, and thus they possess higher sensitivity and can be used for early warning and reconnaissance purposes.

In the future, satellite remote sensing is expected to achieve enhanced spatial resolution, temporal resolution, spectral resolution, and radiometric resolution by make comprehensive use of high-resolution visible light, SWIR, MWIR, and LWIR. This necessitates continuous improvements in the performance of IR detectors, such as low dark current, high sensitivity, and exceptional resolution. Moreover, the detection wavelength needs to be extended to the FIR range, enabling multi-wavelength and hyperspectral detection (Saraf et al., 2008; Sobrino et al., 2016; Khanal et al., 2017; Bhan and Dhar, 2019; Karthikeyan et al.,

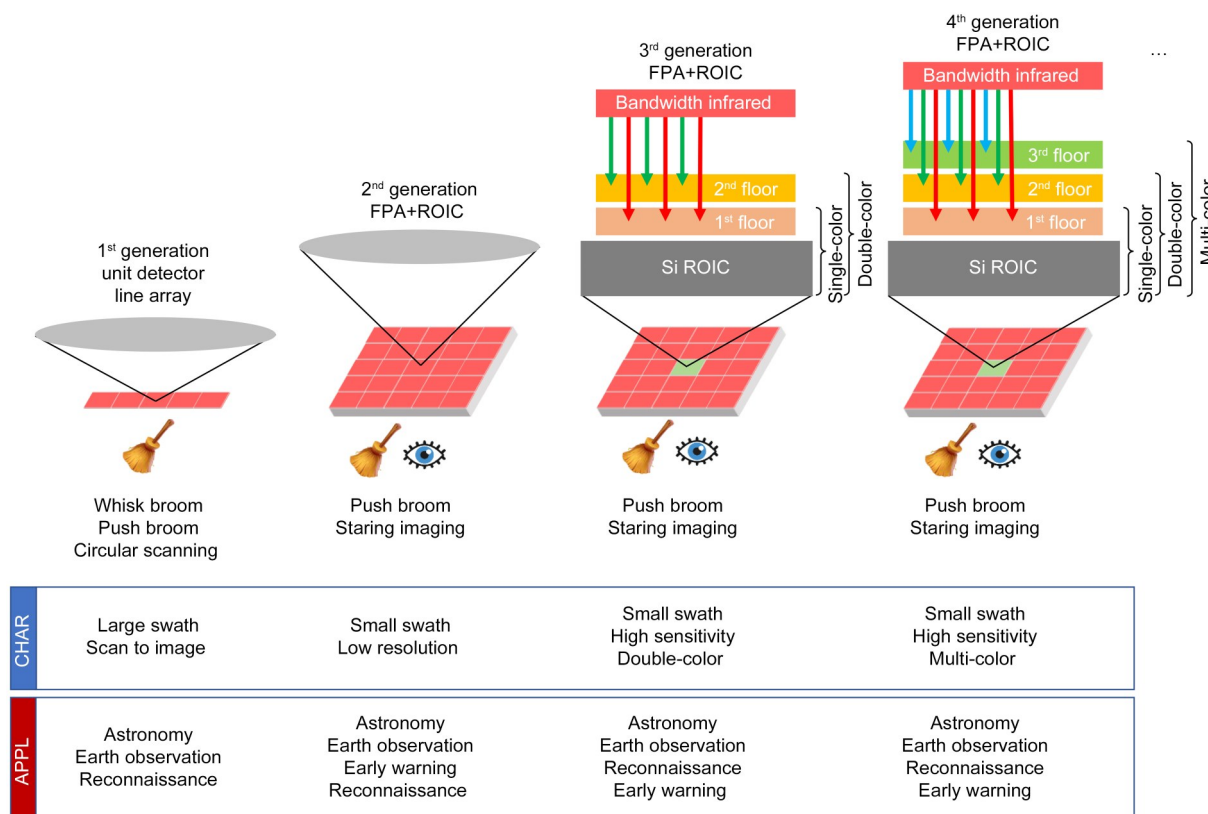


Fig. 5 Evolution and space-based applications of infrared detectors

2020; Yang CH, 2020; Li JD, 2021). The subsequent discussion focuses on the ongoing developments in IR detectors with these advanced features.

1. The main approach to achieving ultra-high spatial resolution in IR detection systems is through the use of large-scale FPA and high-density pixel pitch. Reducing the pixel size effectively reduces the chip size, as well as the size and power requirements of cooling components (Shi WH et al., 2019). In recent years, IR detector arrays with 2 k×2 k (with response wavelengths of 2.3 and 5.2 μm), 3 k×3 k (with response wavelengths of 5.3 and 14.5 μm), and 4 k×4 k (SWIR with 10 and 15 μm pitch) formats have been successfully applied in the aerospace and military fields in the US and France (James, 2019; Ma et al., 2023; Pan et al., 2023; Swindells et al., 2023). With the commercial product, H4RG, the RVS Company has achieved a size of 4096×4096 (1–3 and 3–5 μm spectral ranges, 10/15 μm pixel size) (Fig. 6), and the Lynred Company of France has achieved a size of 1280×1024 (8–14 μm spectral range, 12 μm pixel size) with their commercial product. The double-color IR FPA of the Raytheon

Company in the US has a format size of 1280×720 with the center of pixels of 20 μm (King et al., 2006). A large number of products with a pixel distance of 10 μm have also been released by Lynred, ATTOLLO, Teledyne, and other companies (Reibel et al., 2014; Joshi et al., 2021). Fig. 6 illustrates the timeline and progression of increasing array format and size with the corresponding reduction in pixel size.

2. Avalanche photodiodes (APDs) are the main type of IR detectors capable of achieving high temporal resolution. Notably, the detection sensitivity of HgCdTe APD detectors from the DRS Corporation has reached the single photon level.

3. Hyperspectral is defined as the imaging or sensing of objects or scenes in numerous narrow, contiguous spectral bands. Hyperspectral detectors could identify the object’s spectral band continuously and reflect the fingerprint characteristics of targets. As a result, the detection efficiency of hyperspectral detectors is higher than that of panchromatic or multispectral detectors. The spectral resolution of current advanced hyperspectral detectors in the visible light–SWIR band has reached

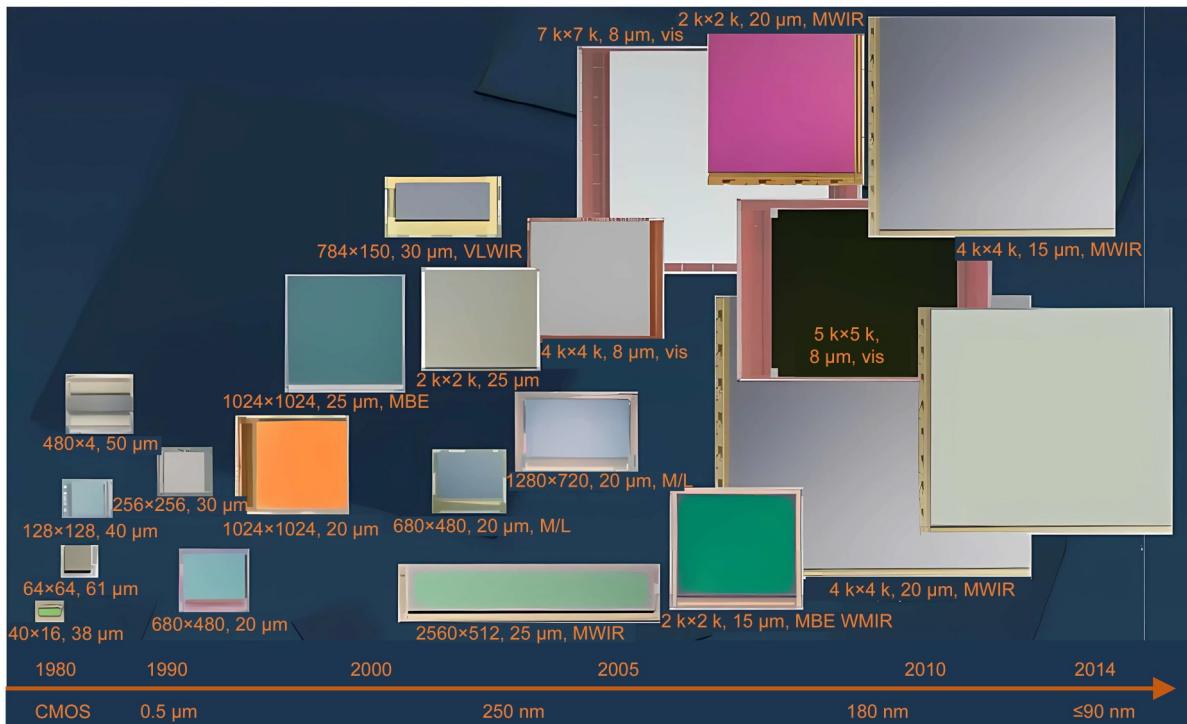


Fig. 6 Focal plane array size progression (Reprinted from Starr et al. (2016), Copyright 2016, with permission from SPIE)

4–10 nm (Lockwood et al., 2006). The Huanjing-1A satellite, Gaofen-5 satellite, Tiangong-2, lunar probe, and Zhuhai-1 satellite launched by China applied hyperspectral IR detectors, and the spectral resolution of Gaofen-5 reached 10 nm in a 1.0–2.5 μm range (Chen JS et al., 2003; Zhao X et al., 2010; Lv et al., 2015; Liu YN et al., 2019).

4. Very-long-wavelength devices with high radiometric resolution have been achieved, e.g., the noise equivalent temperature difference (NETD) of 20 mK, and detectors with a cut-off wavelength of 15–17 μm have been successfully developed. France has developed 384 \times 288 format-sized detectors with a cut-off wavelength of 15.1 μm , and the US has developed IR detectors with a cut-off wavelength of 17 μm (at 80 K). Additionally, the graphene-HgCdTe bilayer-structured detector proposed by Bansal et al. (2018) was able to achieve a cut-off wavelength of 20.6 μm at 77 K.

2.4.2 Progress in emerging MWIR and LWIR technologies

The requirements of cryogenic cooling systems for cooled IR detectors inevitably result in higher operation costs (Li LM et al., 2021). To make IR detectors more economically viable, increasing the working

temperature of cryogenic IR detectors is a direction of effort for many detector researchers (Wu YN et al., 2019). Teledyne has achieved a working temperature of up to 220 K in HgCdTe mid-wavelength devices, and the working temperature of long-wavelength devices has been increased to 160 K (Watson and Zondervan, 2008). In recent years, researchers have developed a series of new detectors to expand their detection wavelength range and improve their working temperature. These include mainly light trap structure IRAPMC, PEIDs, QCIDs-EBE, ICDs, and low-dimensional material IR detectors (Rogalski, 2011). Among them, IRAPMC and QCIDs-EBE have the characteristics of long-wavelength and room-temperature operation. The QCIDs-EBE, invented by Hofstetter in 2002 (Gendron et al., 2004), have low dark current and can work at high temperatures, but have low detectivity and quantum efficiency (Hu et al., 2019; Rogalski et al., 2019b). ICDs, invented by Yang RQ et al. (2010), have a cut-off wavelength of over 7 μm at 320 K, but the detectivity is about 1/100 that of BLIP and needs further improvement.

Theoretical calculations suggest that a barrier blocking nBn structure can effectively reduce the

dark current and enable HgCdTe, InSb, and T2SL detectors to work at higher temperatures, but its fabrication remains challenging (Rogalski, 2011; Shi Q et al., 2022). Lao et al. (2014) proposed a new concept for a detector that uses a thermal carrier for IR detection, the detection wavelength of which can exceed 50 μm , breaking the limitation of the detection wavelength of semiconductor detectors imposed by the semiconductor bandgap (Perera et al., 2016). In 2018, researchers from Georgia State University extended the detection wavelength of semiconductor detectors to 68 μm based on this concept (Chauhan et al., 2018), but such detectors still need to operate at deep cryogenic temperatures. Recently, emerging technologies, such as neuromorphic vision IR chips, flexible IR photodetectors, curved IR photodetectors, and on-chip 3D integrated IR photodetectors, are expected to bring tremendous innovations in the development of IR detectors (Ye et al., 2022). These aim to provide solutions to challenges such as reducing the size and weight of detectors, improving their sensitivity and resolution, and the integration, storage, and processing capabilities on a single chip. These innovations are expected to have a major impact on the space industry and beyond.

3 Developments of space-based IR detection platforms and the applications of IR detectors

IR technology exhibits superior detection capabilities and target identification at night and in adverse weather conditions. This is due to the reduced absorption and scattering of IR light by the atmosphere, compared to the visible spectrum. Consequently, IR detection finds extensive applications in various domains, including medical imaging, meteorology, ocean observation, terrestrial remote sensing, astronomy, and national defense. IR detection sensors on space platforms, such as satellites and telescopes, play an irreplaceable role in capturing thermal radiation information from targets that cannot be achieved by visible light or synthetic aperture radar (SAR) remote sensing techniques (Li JD, 2021).

In land remote sensing applications, IR detection technology finds extensive use in surveying, agriculture, forestry, irrigation, environmental protection,

national land and resources census, and national defense (Saraf et al., 2008; Sobrino et al., 2016; Khanal et al., 2017; Karthikeyan et al., 2020; Yang CH, 2020). Space-based NIR IR remote sensing has been reported to assess the crop area and health of the plantation (Ranganath et al., 2004; Ali et al., 2018; Singh et al., 2020). Specifically, IR detection in the 3.6–12.0 μm range can be used to detect forest fires and analyze the resulting damage (Barducci et al., 2002; Szpakowski and Jensen, 2019; Pérez-Cabello et al., 2021). Furthermore, according to the different absorption and reflection properties of toxic gas, pollution, methane, and water vapor, IR detection serves as an effective approach to meteorological observations and monitoring greenhouse gas emissions and diffusion (Beil et al., 1998; Weeks et al., 2002; Ayasse et al., 2019; Goddijn-Murphy and Williamson, 2019).

In defense applications, space-based platforms help mitigate the limitations posed by the Earth curvature, addressing the blind spots in monitoring and tracking high-speed flying targets, providing a valuable complement to ground radar systems (Fig. 7) (Hirabayashi et al., 2008). Thus, a space-based IR system could be used to track ballistic missiles, hypersonic vehicles, and subsonic vehicles, thereby playing a crucial role in missile early warning systems and military reconnaissance in national defense systems (Smith, 2006; Karim and Andersson, 2013; Wójtowicz et al., 2016; Bhan and Dhar, 2019).

3.1 Space-based IR detection platforms for civilian applications

The role of space-based remote sensing satellites in Earth resource surveying, meteorology, and environmental monitoring has become increasingly prominent with increasing economic development, and IR sensing technologies have greatly promoted the detection abilities in these areas. As a result, many organizations have developed remote sensing satellites that have operated in the IR spectral range since the 1970s, such as Landsat and WorldView satellites from the US, Meteosat from the European Space Agency (ESA), Radarsat from Canada, OKo from Russia, GMS from Japan, and Fengyun (FY) and Gaofen (GF) developed in China. Table 1 presents relevant information, including the IR wavelength bands of selected satellites. In 1996, the Chengdu Institute of Optics and Electronics

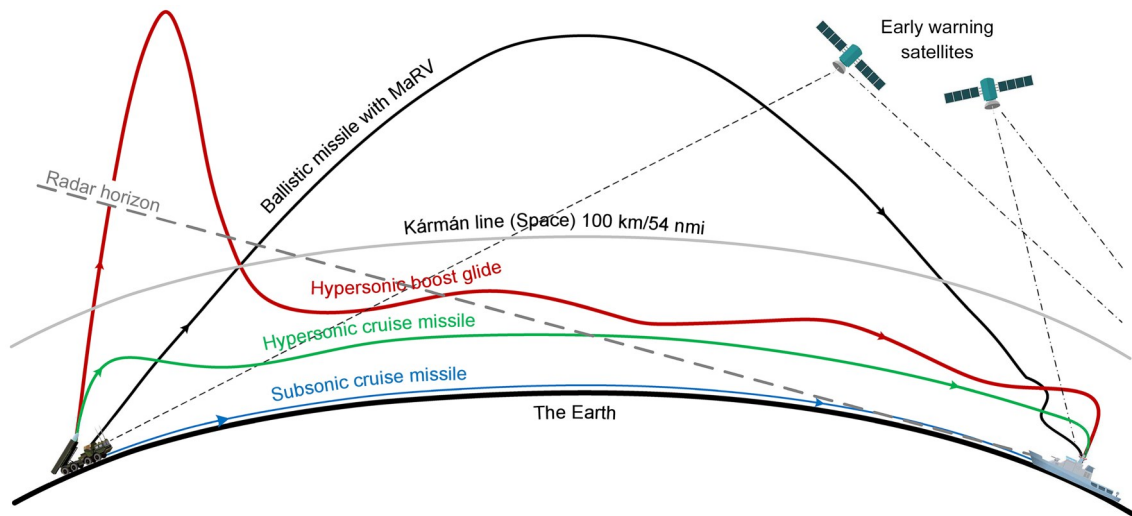


Fig. 7 Comparison of hypersonic strike weapon flight profiles (Robbins, 2019)

Table 1 Parameters of the remote sensing satellites (Barsi et al., 2014; Montanaro et al., 2018)

Mission	Country/Region	Launch time	Orbit/Altitude (km)	Infrared wavelength (μm)	Other property
Landsat 8	US	2013.02	705	1.566–1.651, 2.107–2.294, 10.60–11.19, 11.50–12.51	GaAs QWIP detector at 43 K (Reuter et al., 2015), spatial resolution 30 m (Seenipandi et al., 2021)
Landsat 9	US	2021.09	705	10.0–11.8, 11–12	640×512 GaAs QWIP detector at 43 K (Hair et al., 2018), spatial resolution 30 m (Mill et al., 1994)
GeoEye-2 (WorldView-4)	US	2016.11	617	0.78–0.92	Spatial resolution 0.25 m
WorldView-3	US	2014.08	612×615, 97.98°, Sun-synchronous	1.195–1.225, 1.550–1.590, 2.145–2.185, 2.185–2.225, 2.235–2.285, 2.295–2.365	SWIR resolution 3.7 m (Park H and Choi, 2021)
GMS-5	Japan	1995.03	GEO, 140°E	10.5–11.5, 11.5–12.5, 6.5–7.0	HgCdTe FPA×3, nadir spatial sampling resolution 5.0 km×5.0 km
FY-2C	China	2004.12	GEO	10.3–11.3, 11.5–12.5, 6.3–6.7, 3.5–4.0	Spatial resolution 5.0 km, HgCdTe, NEDT=0.50–0.65 K at 300 K
Meteosat 11	Europe	2015.07	GEO	10.5–11.5, 11.5–12.5	HgCdTe at 85–95 K, resolution 3 km

of the Chinese Academy of Sciences (CAS) successfully pioneered the development of China's first cooled IR optical system. The optical system was cooled by a liquid nitrogen Dewar and operated at about 100 K to maintain the performances of IR detectors in response to 8–14 μm wavelength (Shen et al., 1996). Subsequently, IR detection capabilities were integrated into China's FY satellite series, the China–Pakistan Earth Resources Satellites of the land observation system, the Tianzhou-9B satellite, and the Gaofen-4 satellite (Wu YN et al., 2019; Jiang et al., 2021).

Satellites equipped with IR instruments have been extensively used in various fields, including land and water resource detection, mapping, plantation index analysis, disaster monitoring, desertion monitoring, sea level monitoring, and fishing (Guo HD et al., 2020). A great example is the cooled optical system used for the US Earth observation satellite, Aura launched in 2004, which detects the chemical composition of the Earth atmosphere, including a reflective telescope (operating at 180 K) and filters and relay optics (operating at 65 K), covering the spectral range of 3.2 to

15.4 μm (Abbott et al., 2000). The Fengyun-4 satellite, launched in December 2016, integrates a multi-channel visible and IR scanning imaging instrument, as well as an IR hyperspectral detection instrument, providing remote sensing data sources for the World Meteorological Organization.

3.2 Space-based IR detection platforms for military applications

3.2.1 Developments of Earth observation platforms

Space-based IR detection can be used for high-resolution Earth observation to gather information, and for detecting high-speed targets such as hypersonic vehicles, stealth planes, and ballistic missiles. Many countries have developed high-resolution IR detection systems to enhance their capabilities for Earth observation. Landsat, WorldView, and Keyhole (KH) satellites developed by the US and Helios satellites developed by France are all equipped with high resolution IR systems (Table 2). Moreover, the US, Russia, France, India, Japan, and Israel have established national defense systems based on IR detection for the early identification of high-speed space vehicles, to

enable rapid information analysis, decision-making, and responses (Table 3) (Watson and Zondervan, 2008).

Ballistic missiles have different temperatures and radiation wavelengths at different stages of their flight. As they are boosting through the atmosphere, the center and edge of the flame reach temperature of 1500–2000 K and 600–1000 K are with a peak radiation wavelength in the 2.7–6.3 μm range, respectively (Ding et al., 2014) and radiation power of about 10⁴–10⁶ W/Sr (Zhang X et al., 2010). During the middle flight course, the ballistic missiles are flying in the vacuum of space with the engine turned off, the temperature drops to 200–300 K, the peak radiation wavelength shifts to the 8–15 μm LWIR band, and the radiation power drops to approximately tens of W/Sr (Stair, 1996). When the

Table 2 Typical infrared sensor parameters of high-resolution optical satellites

Mission	Country	Lunch time	Orbit (km)	Resolution (m)
KH-12	US	1989	250–1000	LWIR, 1.0
Helios-2A	France	2004	680	LWIR, 5.0
Helios-2B	France	2009	680	LWIR, 2.5

Table 3 Comparison of the US early warning systems

System	Year	Orbit/Altitude (km)	Wavelength (μm)	Performance
DSP	1970–2007	565×78 970 (DSP-1) 700×39 000 (DSP-2)	SW (2.7 μm)/MW (4.3 μm), double-color	Missile active tail flame detection, with HgCdTe being applied on DSP-12-23
MSX	1996	897×906, 99.16°, Sun-synchronous	4.2–26 μm, Si:As FPA×5 at 11–12 K, 8×192 pixels, solid hydrogen cryostat	1×3° FoV, 90 μrad resolution, mid-course missile warhead discrimination and tracking, missile plume observation, spacecraft acquisition and tracking
SBIRS	2006– 2011–	HEO satellite×4 GEO satellite×6	SWIR (2.7 μm)/MWIR (4.3 μm) (Ni et al., 2006) Triple-color (SWIR, MWIR, HgCdTe) (Chatters and Eberhardt, 2003)	Missile active tail flame global detection Missile early warning and tracking (Rieke et al., 2015)
STSS	1995–	LEO satellite×(20–30)	Visible light, SWIR, MWIR, LWIR, HgCdTe at 40 K (Zhang J et al., 2021)	Globally tracking the launch of ballistic missiles, low temperature reentry and bait vehicle
NFIRE	2007	255×465, 48.2°	LIR HgCdTe (MCT) hybrid, MIR/SIR InSb	Missile phenomenology data collection, test of the laser communication system for missile defense applications
OPIR	2022 2026 (planned) 2028 (planned)	GEO GEO, satellite×2 Polar, satellite×2	LWIR, MWIR, 4 k×4 k focal plane LWIR, MWIR LWIR, MWIR	Wide FoV Developed by Lockheed Martin Developed by Northrop Grumman

missiles reenter the atmosphere or boost, the elevated temperature and the large amount of radiant energy generated by the intense friction will be detected by the geostationary orbit (GEO) and the highly elliptical orbit (HEO) early warning satellite using 2–3 μm band IR detectors. However, the boosting and reentry stages last only about 3%–5% of the total flight time (Lewis and Postol, 1997), so LWIR detection could significantly improve the middle course ballistic missile tracking capability. Therefore, the US developed the DSP (1970–) (Ressler et al., 2008), SBIRS (1992–) (Rieke et al., 2015), STSS (1995–) (Laureijs et al., 2014) (Fig. 7), NFIRE, MSX (Bartschi et al., 1996; Price et al., 1998; Rogalski, 2019), and OPIR systems to enhance the abilities of early warning and tracking of high-speed vehicles. Some of the parameters are shown in Table 3 (Zheng et al., 2008; Bhan and Dhar, 2019). Moreover, Russia developed two generations of IR warning satellites called “Eye” and “Prediction,” and the European Aeronautic Defense and Space (EADS) Company Astrium of France developed two IR warning satellites, called SPIRALE A and B.

DSP and SBIRS can track missiles in the boosting stage effectively, but there is a high risk of missing the target due to the short flight time. Though the mission was ended in 2022, STSS was designed to be the most advanced missile warning and tracking system. It

consists of 20–30 GEO satellites with SWIR, MWIR, and LWIR bands. This enables STSS to detect low temperature targets, capture and track missiles in any stage, classify the boosters, identify the decoys, and evaluate the damage effect (Smith, 2006). STSS provides a 15–30 min early warning time for ballistic missiles and intercontinental ballistic missiles (ICBMs) from anywhere across the globe. Furthermore, if SBIRS works together with STSS, ballistic missiles at any flight stage can be detected and tracked with high accuracy (Fig. 8). Recently, the US Air Force began building a new system called NG-OPIR, which plans to launch the first GEO satellite in 2025 and is designed to replace the SBIRS-GEO satellites and SBIRS-HEO payloads.

3.2.2 Applications of MWIR and LWIR detectors in Earth observation platforms

One of the most challenging applications of IR technology is the monitoring and warning of high-speed moving targets from space. Ballistic missiles, for example, have a surface temperature of around 300 K during the day; the surface temperature decreases to 180 K at night (Sessler et al., 2000). To ensure the signal-to-noise ratio (SNR) and detectivity, the detection bands for midcourse targets are concentrated in the MWIR and LWIR bands (Hoffman et al., 2004; Watson

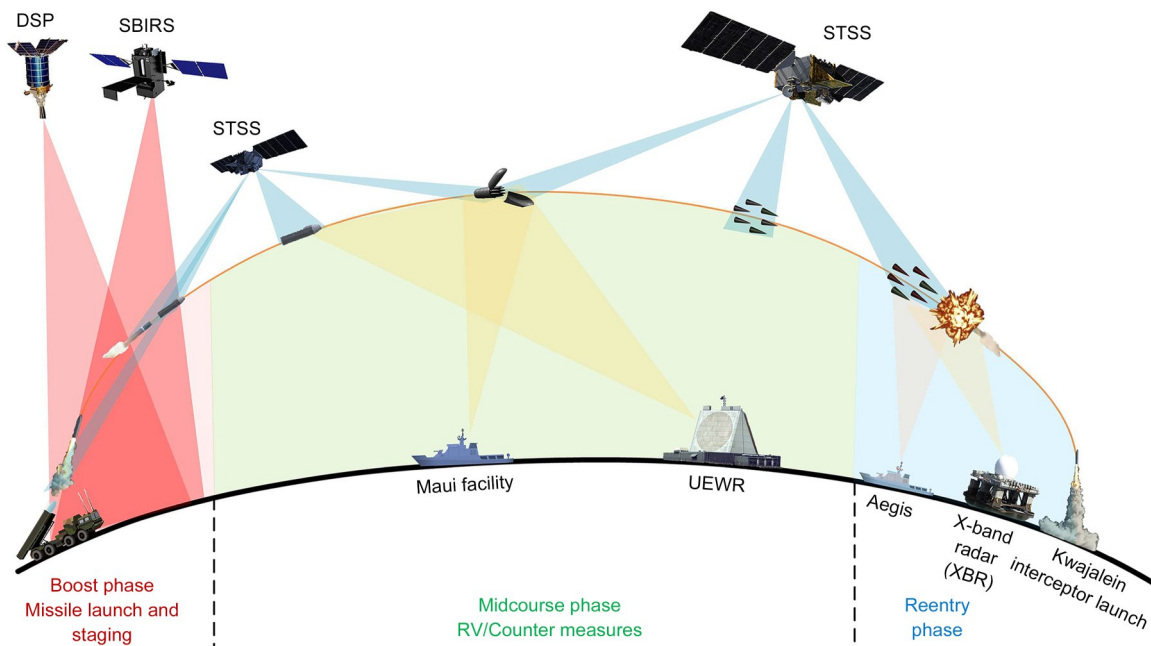


Fig. 8 US DSP, SBIRS, and STSS missile warning programs

and Zondervan, 2008). The US MSX satellite (1996), operating at 35 K, reduced the pixel nonlinearity distortion caused by temperature changes and covered the wavelength band from 0.11 to 28 μm . A wealth of data for the radiant performances of cold and faint targets were obtained by MSX, which provided a basis for the detection band selection of STSS (Mill et al., 1994; Guilmain, 1996). In addition, detectors, such as HgCdTe, were reported to be applied in STSS and N-FIRE satellites, and QWIP was used in the LEO warning satellites of STSS, with an operation temperature of about 40 K. HgCdTe, QWIP, and T2SL are considered the three popular candidates for high-quality MWIR and LWIR detectors for use in space-based Earth observation, the main performances and applications of which are displayed in Table 4. More details are discussed as follows:

1. HgCdTe is characterized by a high quantum efficiency ($\geq 80\%$), good responsiveness, and multi-spectral detection. The cut-off wavelength of Hg_xCd_{1-x}Te can be tuned by adjusting the components to cover 1–20 μm (Rogalski, 2009). Thus, HgCdTe is popularly used in remote sensing, astronomy, and healthcare;

the development trend is multi-color and large array. Although the fabrication technology of the HgCdTe detector has gradually matured in recent years, it comes with high technical barriers. There are only a few companies capable of developing and producing high-performance HgCdTe FPAs globally. HgCdTe FPAs have format sizes that have developed from 1 k \times 1 k to 4 k \times 4 k pixels at 2.3, 5.0, and 14.5 μm bands to as large as 8 k \times 8 k with pixel size ranging from 8 to 27 μm (Hall et al., 2004; Figer et al., 2018; James, 2019; Li JD et al., 2021; Swindells et al., 2023), while the maximum FPA size HgCdTe detector, at the 19 μm band, is only 320 \times 256 (at 50 K) due to fabrication difficulties.

2. QWIP detectors exhibit good uniformity, radiation resistance, high sensitivity, and excellent large array consistency, but relatively low quantum efficiency. Therefore, QWIPs are suitable for medical imaging, astronomy observation, ballistic missile monitoring, and reconnaissance (Tidrow and Dyer, 2001). QWIPs need to operate at low temperatures to achieve the optimal detectivity at 77 K for the IR band and at 35 K for the FIR and terahertz bands. Fig. 9 shows images of rocket launch captured by LWIR QWIP FPA detectors

Table 4 Detectors and performances (Abbott et al., 2000; Rogalski, 2009, 2019)

Item	HgCdTe	QWIP	InAs/GaSb type-II SL	InAs/InAsSb type-II SL
Type	Photovoltaic	Photoconductive	Photovoltaic	Photovoltaic
Spectral response	Wideband adjustable	Narrowband	Wideband adjustable	
Quantum efficiency (QE)	$\geq 80\%$	$\leq 10\%$	50%–60%	40%
D^* (10 μm , FoV=0)	$3 \times 10^{12} \text{ cm} \cdot \text{Hz}^{1/2} \cdot \text{W}^{-1}$	$10^{10} \text{ cm} \cdot \text{Hz}^{1/2} \cdot \text{W}^{-1}$	$1 \times 10^{12} \text{ cm} \cdot \text{Hz}^{1/2} \cdot \text{W}^{-1}$	$4 \times 10^{11} \text{ cm} \cdot \text{Hz}^{1/2} \cdot \text{W}^{-1}$
Advantage	High efficiency and D^* , multi-spectral	High uniformity	High operation temperature and uniformity, low dark current	
Maximum array size and peak wavelength	8 k \times 8 k (Figer et al., 2018), 4 k \times 4 k, 5 μm (Tan and Mohseni, 2018), 320 \times 256, 19 μm at 50 K (Joshi et al., 2021)	128 \times 128, 14.9 μm (Rogalski, 2009)	1280 \times 1024, 12 μm (Dehzangi et al., 2019)	
Disadvantage	Cryogenic needed for FIR, poor uniformity	Low efficiency and D^* , cryogenic needed	Lower QE than HgCdTe	
Space application	2009, US, STSS, 40 K; 2007, N-FIRE, 40 K; SBIRS, 43 K; 1995, GMS-5; 2004, FY-2C; 2015, Meteosat-11, 85–95 K	2013, Landsat-8; 2021, Landsat-9	FPA for space applications developed by Jet Propulsion Laboratory (JPL), Sweden, etc.	

(Goldberg, 2003; Rogalski, 2003b). Additionally, it was reported that QWIP has been employed by the famous Landsat-8/9 satellites developed by the US (Hickey et al., 2018; Jhabvala et al., 2020).

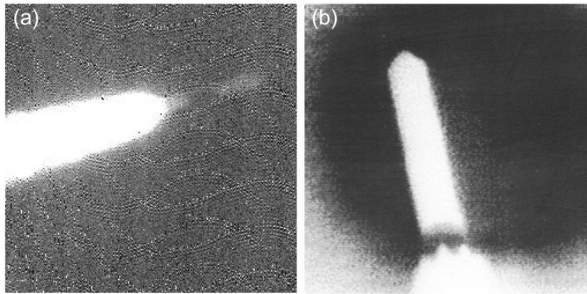


Fig. 9 Images of rocket launch captured by QWIP detectors: (a) image of a Delta-II launch vehicle taken with the LW QWIP radiance during the launch (Rogalski, 2003b); (b) raw LWIR image showing Atlas 5 vehicle during the launch (Goldberg, 2003)

3. T2SL material can provide double-color and multi-color detection capabilities in the 3–30 μm wavelength range by adjusting the band structure and band gap. Studies have shown that the T2SL detector has advantages of high quantum efficiency, high sensitivity, and low dark current, and can operate at higher temperatures (Manurkar et al., 2010; Zheng et al., 2010; Ivanov et al., 2019). Thus, T2SL is considered the most promising alternative to HgCdTe materials in the future (Alshahrani et al., 2022). Currently, the maximum size of the T2SL FPA is 1280 \times 720, and the wavelength of 12.5 μm has been achieved for the FPA device. However, most of the current applications focus on the high temperature range. In Japan, a 4 k \times 4 k (at 2.5 μm) T2SL FPA has been developed as a substitute for the HgCdTe detector operating at 210 K. In the US, a 14.3 μm (at 77 K) T2SL FPA achieved a detectivity of 4×10^{10} J and a quantum efficiency of 37%, which are comparable to those of the most advanced HgCdTe operating under the same conditions. Recently, the T2SL FPA with a wavelength of 14.5–16.5 μm with the aim of providing weather forecasts and atmospheric warnings is under development by IRnova in Sweden (Höglund, 2017; Pipher et al., 2021). Chinese research institutions, such as the Institute of Semiconductors of the CAS, have developed LWIR detectors of 640 \times 512 based on T2SL, with cut-off wavelengths of 10 and 16 μm (Han

et al., 2018). The Shanghai Institute of Technical Physics of the CAS has developed InAs/GaSb T2SL IR detectors with a wavelength of 12.5 μm (Shang et al., 2021). However, the cooled T2SL detector has not been applied in space and suborbital vehicles yet (Pipher et al., 2021).

3.3 Space-based IR detection platforms for astronomy applications

3.3.1 Developments of IR astronomy observation platforms

IR detection is crucial for studying the origin of planets, stars, galaxies, and the universe. These targets are extremely far away, and their radiation is excessively weak. Thus, high sensitivity and resolution IR detectors are essential for their detection. For instance, the first detected brown dwarf had a temperature of about 1000–2000 K, which can be detected using only IR methods (Bhan and Dhar, 2019). The temperature of M/L type brown dwarfs is about 1500–3000 K, with a radiation wavelength of around 1.2 μm . The T-type brown dwarf has a temperature of about 800 K, with a radiation wavelength of about 4 μm , while the radiation wavelength for some galaxies and stardust is about 60 μm (Young, 2002). In general, space-based astronomical observations can cover the IR detection wavelength range of 20 to 800 μm (Rieke, 2007; Farrah et al., 2019). To meet the demands of detecting these faint and distant objects, several scientific satellites and telescopes with IR bands have been developed by the US, Europe, and Japan (Rogalski, 2019), as displayed in Table 5. Most of these telescopes operate in the liquid helium or liquid neon temperature ranges, and the single aperture FIR (SAFIR) equipment designed for the Calisto telescope achieved a detection wavelength of up to 1000 μm .

The US launched its first IR astronomical satellite, the Infrared Astronomical Satellite (IRAS), in the 1980s, followed by the Hubble Space Telescope (HST), Wide-Field Infrared Survey Explorer (WISE), and Space Infrared Telescope Facility (SIRTF). In 2021, JWST was launched, equipped with an IR band that covers 0.6–28 μm and several advanced instruments including an NIR camera, an NIR spectrometer, a mid-infrared camera, and a fine guidance sensor (Ressler et al., 2015; Rieke et al., 2015).

Table 5 Selected space telescopes and instruments

Mission	Year	Wavelength (μm)	Aperture (m)	Cooling	IR detector material
IRAS	1983	8–120	0.57	Superfluid helium	Si:As, Si:Sb, Ge:Ga, Si:Ga
IR Space Observatory (ISO)	1995	2.5–240	0.60	Helium	Si:As (1 \times 12)
Hubble Near-Infrared Camera and Multi-Object Spectrometer (NICMOS) (Zhao W et al., 2020)	1997	0.8–2.4	2.4	Nitrogen, later cryocooler	HgCdTe (256 \times 256)
Spitzer Space Telescope	2003	3–180	0.85	Helium	Si:As (128 \times 128) Si:As (256 \times 256) Ge:Ga (32 \times 32)
SOFIA	2005	1–655	2.5	He ³ /He ⁴ , ADR	Si:As (128 \times 128) Ge:Ga (16 \times 25)
Akari	2006	5.7–7.8	0.67	Liquid helium, stirling-cycle mechanical refrigerator	Si:As (256 \times 256) Ge:Ga (3 \times 20)
Hubble Wide Field Camera 3 (WFC3)	2009	0.2–1.7	2.4	Passive and thermo-electric (Laureijs et al., 2014)	HgCdTe (1024 \times 1024)
Herschel Space Observatory	2009	55–672	3.5	Helium	Ge:Ga (16 \times 25)
Single Aperture Far-Infrared (SAFIR); Cryogenic Aperture Large Infrared Space Telescope Observatory (CALISTO)	2015	5–1000	5–10	Passive cooling, helium cooler	HgCdTe (256 \times 256)
WISE	2009	2.8–26	0.4	Two-stage solid hydrogen (8.3–17.0 K)	Si:As (1024 \times 1024) HgCdTe (1024 \times 1024)
JWST (Gáspár et al., 2021)	2021	0.6–28.5	6.5 (Si:As), 37 (HgCdTe)	Passive cooling, cryocooler	Si:As (1024 \times 1024) HgCdTe (2048 \times 2048)
SPICA (Roelfsema et al., 2018; Shinozaki et al., 2020)	2032 (planned)	12–36 (SMI) 35–230 (SAFRI) 100, 200, 350 (B-BOP) 35–430 (BLISS)	2.5	Stirling, J-T, ADR, sorption	Si:Sb (1 k \times 1 k) Si:As (1 k \times 1 k) Ge:Ga (64 \times 64) (planned)
Origins Space Telescope (Roellig et al., 2020; Wiedner et al., 2021)	2032 (planned)	2.8–20.0 (MISC-T)	15	Active, multi-stage cryocoolers needed	HgCdTe (2 k \times 2 k) Si:As (2 k \times 2 k) (needed)

ESA launched the second IR astronomical satellite in the world, the Infrared Space Observatory (ISO), in 1995. It covered a wavelength range of 24–240 μm and aimed to detect gas molecules and dust clouds with temperatures below 10 K (Kessler, 1989, 1993; Singer et al., 1991). Subsequently, the ESA developed the Herschel Space Telescope (Herschel) and the Euclid Space Telescope with IR instruments (Laureijs et al., 2014). Japan has also made significant contributions to

advanced IR astronomical satellites, including IRTS, ASTRO-F, AKARI, and the latest SPICA (Ishihara et al., 2003; Onaka et al., 2010; Nakagawa et al., 2012).

3.3.2 Applications of MWIR and LWIR detectors in space-based astronomy observations

The IR detection instruments of telescopes, including radiant meters, imaging ends, and spectral meters, typically use cooled IR detectors to accomplish their

objectives (Yin et al., 2013). McNutt established the first cryogenic IR optical system in 1996 for telescopes using InSb and Au:Ge detectors, which were cooled to 80 K by liquid nitrogen (N_2) (Harwit et al., 1966). The cryogenic IR instrument IRAS, onboard the first optical astronomy satellite jointly designed by the US, UK, and the Netherlands in 1983, operated at 4 K and covered the 8–12 μm wavelength range (Harland, 2021). In the high-performance IR astronomy observation telescopes established by the US, Europe, and Japan, non-intrinsic high sensitivity Si detectors operated at temperatures ranging from 0.3 to 60 K, covering the detection range from SIR to FIR. These telescopes are outlined in Fig. 10.

In astronomical applications, HgCdTe, Si:As, and Ge:Ga are the most popular IR detector materials

(Fig. 11). Built on the heritage of the detectors used in the Spitzer instruments such as WISE, MSX, and Akari, the Si:As IBC detector arrays for MIRI in JWST have a larger 1024×1024 format, covering the 5–28 μm band, with good quantum efficiency and low dark current, while operating at about 7 K (Rieke et al., 2015). In addition, Si:As detectors have been used for ISO, WISE, SOFIA, and MIMIZUKU, with an operation temperature of around 10 K. The detection wavelength of Ge:Ga is 40–120 μm , which makes it suitable for Herschel, SPITZER, SOFIA, AKARI, and SPICA. Moreover, Olsen (1997) and Hanaoka (2016) verified that Ge:Sb has a larger cut-off wavelength compared with Ge:Ga (Pipher et al., 2021). In astronomy applications, HgCdTe detectors are used for mid- and short-wavelength detection. For instance,

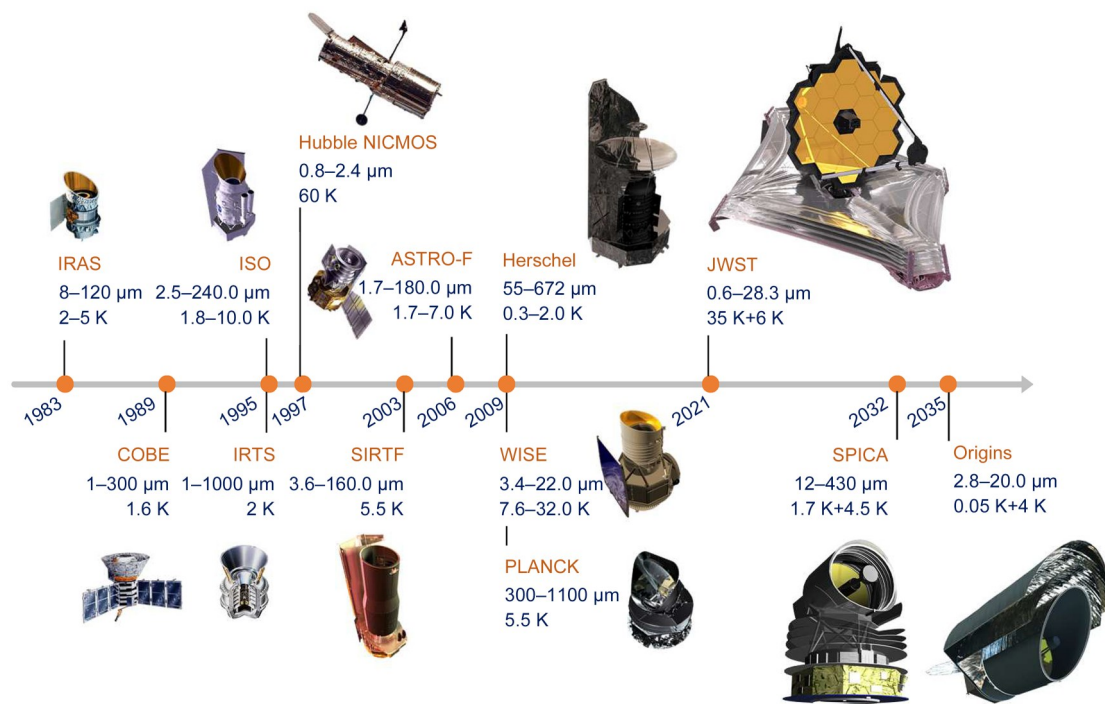


Fig. 10 Development of cooled infrared systems onboard space telescopes

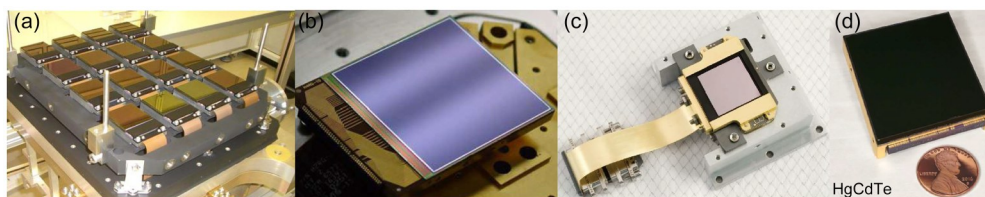


Fig. 11 Large IR FPAs: (a) Hawaii-4RG-10 (4096×4096 , 10-mm pitch), used for astronomy observations (Rogalski, 2010); (b) $16\,248 \times 2048$ HgCdTe arrays assembled for the VISTA telescope (Rogalski, 2017); (c) IR detectors applied on JWST (Ressler et al., 2015); (d) HgCdTe long-wavelength detector ($\lambda > 10 \mu\text{m}$) used in NEOSM (Roellig et al., 2020)

JWST used HgCdTe to cover 0.6–5.0 μm and 0.6–2.5 μm wavelength bands (Rieke, 2007).

3.4 Summary of the requirements of IR detectors in space-based applications

The overall development trajectory of IR detectors can be categorized into four stages as outlined in Fig. 5. The first-generation IR detectors comprise unit detectors and line arrays with a lower pixel count, and are primarily employed in optical–mechanical scanning. Moving on to the 2nd generation, IR FPA detectors were developed and have been used in push-scan applications. The 3rd generation IR PFAs come with a larger format size, enabling their use in staring type applications. These have evolved from small format sizes to 1000×1000, 2048×2048, and 4096×4096, with the largest now being 8192×8192. Additionally, the pixel sizes have decreased from 15, 10, and 8 μm to the current 5 μm , while the frame rate has increased from 1 to 10 kHz (Ye et al., 2022; Pan et al., 2023). Presently, the 4th generation IR detectors are under development and are aiming for multi-dimensional detection, chip integration, and intelligent applications.

Furthermore, as we gather insights from the preceding discussions, it becomes evident that the requirements for IR detectors used in civilian satellite remote sensing, military satellite remote sensing, and space-based astronomy platforms differ according to the intended applications and mission-specific technical needs. In summary, the general characteristics of IR detectors used in these different application domains are outlined as follows:

1. For civilian applications of space-based IR detection, the development of IR detectors prioritizes high spatial resolution, broad spectral range, high sensitivity, and low noise. The detectors should be sensitive to a broad range of IR wavelengths, ranging from NIR to LWIR, to provide a comprehensive understanding of Earth's different objects and phenomena. The detectors should also be able to provide high-quality images with high spatial resolution, which requires a high level of sensitivity and low noise.

2. For military applications of space-based IR detection, devices with long-range detection capabilities and high sensitivity are preferred for surveillance, early warning, and defense purposes. The detectors

should be able to detect specific features or various objects of interest from long distances and through various atmospheric conditions. A cryogenic environment is typically required to ensure high sensitivity and high performance.

3. For astronomy applications of space-based IR detection, IR detectors are required to have high sensitivity, broad spectral range, and low noise, to detect very faint IR radiation over a broad range of wavelengths emitted by celestial objects. Additionally, many space-based astronomy platforms require cryogenic cooling systems to reduce thermal noise and improve the sensitivity of the detectors, which poses additional technical challenges for detector design and thermal management.

In general, the development requirements for IR detectors for space use vary widely based on the intended applications and the technical design of the specific mission. However, high sensitivity, low noise, and long operation range are common requirements for IR detectors used for civilian and military remote sensing and space-based astronomy platforms.

4 Requirements of the MWIR and LWIR detectors to enhance future space-based IR detection

4.1 Key performance indicators and their interconnections of the space-based IR detection system

A typical configuration for a space-based infrared detection system includes several key components: an optical system, IR FPA detectors, an opto-mechanical system, electric circuits, and a thermal control system. These components collaborate to guarantee the proper functioning of not only the IR detectors and the optical system but also the entire IR detection system, enabling remote target detection from space platforms.

The primary performance indicators used to evaluate a space-based IR detection system include parameters such as the modulation transfer function (MTF), swath, ground sample distance (GSD), operation range, NETD, SNR, and the spectral characteristics. These indicators serve as the fundamental requirements for designing an effective IR detection system.

Based on these performance indicators, one can determine the specific requirements for IR detectors and obtain the design parameters for the optical system and its supportive systems. The main design parameters for the optical system include field of view (FoV), focal length, optical aperture, and F number (which is determined by the focal length and optical aperture). The supportive systems should take into account factors such as the optical system MTF, operational noise, operation temperature, and the spectrum characteristics. The selection of IR detectors should consider factors including detector MTF, detectivity, noise, detector spectral response, format size, and pixel size. The relationships between these key performance indicators in designing a space-based IR detection system are summarized and illustrated in Fig. 12. Referring to Fig. 12, we can discern how an IR detector characteristic impacts the performance indicators of the IR detection system and determine the design parameters required to meet the IR detection system specifications.

4.2 Comprehensive evaluation of the performances of MWIR and LWIR detectors for space application

As discussed in Section 4.1 and illustrated in Fig. 12, the key performance indicators for a comprehensive evaluation of space-based IR detection systems include GSD, operational range, NETD, SNR, and spectral characteristics (Li JD, 2021).

SNR plays a crucial role in characterizing the radiation features of a remote sensing satellite and is influenced by various factors within the optical system,

including detector and electrical circuit noise. On the other hand, dynamic range, which is not included in Fig. 12, pertains to the maximum and minimum input signal ranges that remote sensing satellites can effectively handle, and it is impacted by detector performance, noise, and other factors. To detect targets with varying radiation intensity, detectors with a high dynamic range are required.

GSD is a measure of the spatial resolution of an imaging system and is defined as the distance on the ground represented by each pixel in the image, which is influenced mainly by the orbital altitude, focal length, and pixel size.

$$GSD = \frac{S}{\cos \theta} \cdot \frac{p}{f}, \tag{2}$$

where p is the pixel distance, f is the focal length, and S is the detection distance between the detector and targets, depending on the orbital altitude of the Earth orbital spacecraft.

In general, a higher altitude allows an IR imaging system to cover a larger area, but at the expense of reduced spatial resolution. Therefore, detectors with a larger operation range are helpful in improving the imaging quality. The operation range is defined as the maximum distance at which the IR imaging system can detect and identify a target, as described in Eq. (3) (Hudson, 1969):

$$R^2 = \frac{I_t \tau_{opt} \eta \tau_{air} A_{opt} D^*}{\sqrt{A_d \Delta f} SNR_{min}}, \tag{3}$$

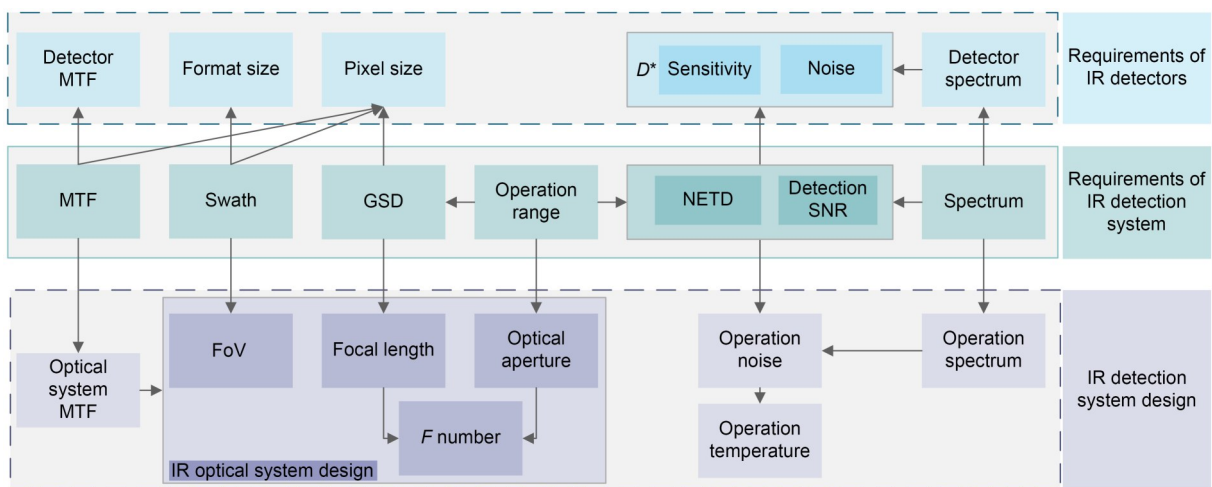


Fig. 12 Interconnections between the performance indicators of infrared detectors and detection systems

where D^* is the specific detectivity, A_d is the format size of the detector, Δf is the noise equivalent bandwidth, A_{opt} is the entrance area of the camera, τ_{air} and τ_{opt} are the transmittances of the atmosphere and optics respectively, I_t is the radiation intensity of the target, η is the system efficiency, and SNR_{min} is the minimum SNR of the optical system.

Eq. (3) reveals that the square of R is proportional to D^* , whereas the research results from Sclar (1984) and Rogalski (2011) indicate that D^* and cut-off wavelength could be greatly improved by reducing the operation temperature of the detector, thus leading to an increase in the detection distance accordingly. For example, cooling an HgCdTe detector from 80 to 40 K can increase the detection distance by up to six times, which in turn can help reduce the required diameter of the IR optical camera and the number of satellites needed to cover the same observation area.

Another benefit of reducing the operation temperature of a detector is to enhance the thermal sensitivity, which can decrease the NETD. NETD is a measure of the minimum temperature difference that can be detected. The improvement in thermal sensitivity can enable more precise measurements and observations of the target objects, making it an essential factor in the design and operation of IR detectors (Rogalski, 2019; Li JD et al., 2021).

$$NETD = \frac{4 \sqrt{A_d \Delta f}}{\frac{dM}{dT} \Omega D_0^2 \tau_0 D^* \delta}, \quad (4)$$

where Ω is the instantaneous stereo FoV, D_0 is the aperture of the optical system, τ_0 is the efficiency of the optical system, and δ is the process factor. Eq. (4) reveals that NETD is proportional to the detector format size and is inversely proportional to D^* .

Eqs. (3) and (4) indicate that for the IR system of an Earth orbit remote sensing satellite, a larger detector format size will improve D^* and NETD, while a smaller pixel distance will reduce GSD at a specific orbit. These factors suggest the existence of an optimal resolution for the optical system. By considering these trade-offs, designers can achieve a balance between the detector format size, pixel distance, and GSD, resulting in a system that provides the best possible performance for its intended application.

Observing targets from space platforms requires IR detectors with high sensitivity, high responsivity, and low NETD to detect low-temperature objects with high resolution and achieve hyperspectral capabilities. This necessitates the use of long-wavelength and very-long-wavelength IR detectors with higher radiometric resolution. Additionally, it is essential to minimize dark current noise and background stray light radiance when operating the IR system in a cryogenic environment (Sanders, 2004; Schwalm et al., 2005; Hirabayashi et al., 2008; Rodriguez, 2017; Park S et al., 2019). Researchers have proposed Eq. (5) as an approximate way to evaluate the operation temperature of an IR detector (Long D, 1977), which indicates that the operation temperature should be decreased as the cut-off wavelength increases.

$$T_{max} = 300/\lambda_c, \quad (5)$$

where λ_c is the cut-off wavelength (in μm).

For instance, mid-wavelength HgCdTe (Rogalski, 2005), Ga/Sb/InAs (Grein et al., 1995; Bartschi et al., 1996; Lin et al., 2000; Zheng et al., 2008; Rogalski, 2019), and InSb (Kimukin et al., 2004) detectors require an operation temperature of 77 K, while long-wavelength Si:As BIB arrays (Keller et al., 2000) should operate at 4.2 K to achieve D^* values of 10^{10} – 10^{11} J (Rodriguez, 2017). A popular study showed that D^* of HgCdTe and the T2SL can be theoretically increased by up to three orders of magnitude (Bajaj et al., 2007; Rogalski, 2009). The research conducted by the US Air Force has revealed that the detectivity and detectable wavelength range of QWIP detectors can be significantly improved by lowering the operation temperature from 65 to 40 K, while the detectivity of HgCdTe detectors can also be improved by reducing the operation temperature from 80 to 40 K (Roberts and Roush, 2007). We investigated the relationship between D^* , pixel distance, and the maximum detection distance based on Eqs. (3) and (4). The IR system parameters used for calculation are listed in Table 6, and the values of D^* of HgCdTe detectors are referenced from the literature (Roberts and Roush, 2007). The results shown in Fig. 13 indicate that reducing the operation temperature can significantly increase the detectivity. Moreover, a smaller pixel size and a lower NETD can significantly extend the maximum detection distance (operation range).

Table 6 Values of the IR system parameters we used to calculate the maximum detection distance

Symbol	Description	Value	Unit
D_0	Aperture of the optical system	1	m
D^*	Specific detectivity of HgCdTe at 80 K, 40 K	10^{11} – 10^{12} , 10^{13} – 10^{14}	$\text{cm}\cdot\text{Hz}^{1/2}\cdot\text{W}^{-1}$
I_t	Radiation intensity of the target	500	W/Sr
f	Focal length	5	m
SNR	Signal-to-noise ratio	10	
Δf	Noise equivalent bandwidth	15.7	s^{-1}
τ_{air}	Transmittance of the atmosphere	0.8	
τ_{opt}	Transmittance of optics	0.8	

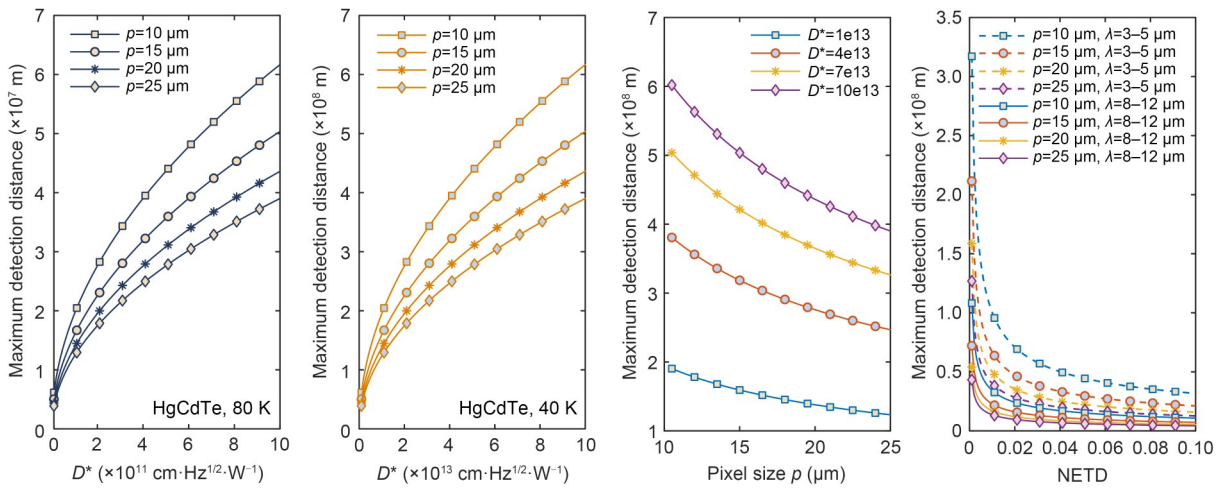


Fig. 13 Relationship between D^* , pixel distance, temperature, wavelength, and the maximum detection distance of an infrared system

The use of smaller pixels can increase the functionality of imaging systems (Kopytko and Rogalski, 2022), but it is worth noting that a smaller pixel size does not necessarily guarantee a better performance. The pixel size in an imaging system affects the MTF and the ability to resolve fine details in the image. If the pixel size is too small, the captured image may contain excessive noise induced by minority carrier diffusion, or be limited by the diffraction effects, as defined by the Nyquist–Shannon sampling theorem (pixel size= $\lambda f/2$). When the pixel size is too large compared to the diffraction limit, MTF of the detector is affected, leading to a reduced spatial resolution. To strike a balance, the pixel size should be chosen to ensure that it adequately samples the optical system, allowing for high-resolution imaging while considering the diffraction limit and other factors that can affect the MTF of the system. For example, the wavelength diffraction limit is approximately 3 μm for mid-wavelength

IR and approximately 8 μm for long-wavelength IR. A smaller pixel size in an imaging system does not necessarily guarantee a better performance.

4.3 Future development requirements of MWIR and LWIR detectors for high-resolution Earth observation

Considering the ongoing developments in IR detection technology and the evolving demands from space-based Earth observation, the imaging resolution and target recognition capabilities of space-based Earth remote sensing will continue to increase. Consequently, the performance standards for IR detectors are expected to rise. However, it is worth noting that the current IR detector technologies in the short-wave band are relatively mature, whereas the development of IR detectors in the mid- and long-wavelength bands faces challenges in realizing large array sizes, high detectivity, effective blind cell rate control, and high-density

integration. These challenges pose several obstacles to the developments of advanced IR Earth observation platforms:

1. There is an urgent demand for IR detectors with larger format size, smaller pixel size, low noise, high sensitivity, and a wide dynamic range to enable the development of high-performance optical remote sensing systems in space. However, currently the manufacturing of high-quality large format MWIR and LWIR FPAs remains a significant challenge. Only a few manufacturers worldwide are capable of providing highly qualified IR FPAs, particularly for operations in the MWIR and LWIR bands.

2. To maintain the performance of these high-quality IR FPAs, cryogenic cooling is necessary. However, cryogenic cooling technology operating below 35 K faces several challenges, including low efficiency, difficulties in maintaining a compact form for multi-stage cryocoolers, and increased sensitivity to impurities in the working fluid.

3. Although there are new types of IR materials with potential suitability for MWIR and LWIR FPAs, the manufacturing presents challenges in terms of meeting the needs of various applications.

As a result, future studies of IR detectors for space applications should prioritize the following areas:

1. IR detectors with extremely large array sizes and small pixel sizes should be developed to improve the integration of high-density IR detection arrays, reduce the detector size and power of the refrigeration system, and enhance the spatial resolution of the imaging system, image quality, and target recognition ability.

2. The spectrum of future IR detectors should be expanded to mid-wavelength, long wavelength, and very long wavelength with a high temperature resolution of mK and high sensitivity, to improve the radiometric resolution and space detection capabilities of low temperature moving targets and distant astronomical targets.

3. Further advancements in IR detectors can be achieved by reducing the dark current and noise to enhance sensitivity and detectivity and increase the detection distance and spectral resolution, while achieving higher detection efficiency and target recognition ability at the same orbital height.

4. High frame rate detectors and high dynamic range (HDR) detectors with fast response capabilities

are necessary to improve the temporal resolution of the detection system.

5. Innovative technologies should be applied to develop the next generation IR detectors. These include multi-dimensional information fusion imaging, on-chip intelligence, on-chip sensing, storage, and processing ability, to facilitate the intelligent development of space remote sensing and its high-efficiency applications.

5 Conclusions

We reviewed the features, development, and applications of MWIR and LWIR detection technologies for Earth observation, national defense, and astronomy observations. The importance of MWIR and LWIR detection in these areas is analyzed with a special emphasis placed on space-based Earth observation. Future space-based observation applications, such as the IR detection of supersonic vehicles and missiles and astronomy observations, require higher spatial, temporal, radiometric, and spectral resolution from satellite remote sensing systems, which in turn necessitates high-performance IR detectors. This poses new challenges and development trends for mid- and long-wavelength IR detectors. Therefore, efforts should focus on studying high-performance MWIR and LWIR detectors to have space detection capability and the ability to explore the margins of space, which will support future space resource exploration and space policy formulation as well.

To achieve this, future IR detectors must have a detection spectrum that expands to mid-wavelength and long or very long wavelength, with a large integrated format size and a smaller pixel size. Moreover, to reduce the dark current, achieve background-limited performance, and improve the sensitivity and detectivity of the detectors, a cryogenic temperature environment remains the main approach to ensuring these high performances, although the advancement of HOT detectors, artificial intelligence, and artificial microstructure technologies has promoted the development of IR detectors. In the context of weak target detection and low background conditions, HOT IR detectors cannot replace high-performance cooled MWIR and LWIR detectors due to the considerable background radiation they generate. Thus, HgCdTe, QWIPs, and T2SL detectors are

still the representatives of high-performance mid- and long-wavelength IR detectors suitable for space applications. Nonetheless, it is expected that in the future, a new generation of IR detectors with multi-dimensional information fusion imaging, on-chip intelligence, and on-chip sensing-storage-processing features will further enhance IR detector technologies.

Contributors

Yuying WANG collected, analyzed, and summarized the literature, and drafted the paper. Xiang LI, Hezhi SUN, and Jindong LI helped organize the paper. Hezhi SUN and Xiang LI processed the figures and calculations. Yuying WANG, Hezhi SUN, and Xiang LI revised and finalized the paper.

Conflict of interest

All the authors declare that they have no conflict of interest.

References

- Abbott JL, Thorndyke P, Catanzaro BE, et al., 2000. Light-weight thermally conductive composite optical bench for the tropospheric emission spectrometer (TES) interferometer. *Proc SPIE 4004, Telescope Structures, Enclosures, Controls, Assembly/Integration/Validation, and Commissioning*, p.600-611. <https://doi.org/10.1117/12.393953>
- Ali HM, Rasib AW, Hamid NRA, et al., 2018. Determination of rubber-tree clones leaf diseases spectral using unmanned aerial vehicle compact sensor. *IOP Conf Ser Earth Environ Sci*, 169(1):012059. <https://doi.org/10.1088/1755-1315/169/1/012059>
- Alshahrani DO, Kesaria M, Anyebe EA, et al., 2022. Emerging type-II superlattices of InAs/InAsSb and InAs/GaSb for mid-wavelength infrared photodetectors. *Adv Photon Res*, 3(2):2100094. <https://doi.org/10.1002/adpr.202100094>
- Ayasse AK, Dennison PE, Foote M, et al., 2019. Methane mapping with future satellite imaging spectrometers. *Remote Sens*, 11(24):3054. <https://doi.org/10.3390/rs11243054>
- Bajaj J, Sullivan G, Lee D, et al., 2007. Comparison of type-II superlattice and HgCdTe infrared detector technologies. *Proc SPIE 6542, Infrared Technology and Applications XXXIII, Article 65420B*. <https://doi.org/10.1117/12.723849>
- Bansal S, Sharma K, Jain P, et al., 2018. Bilayer graphene/HgCdTe based very long infrared photodetector with superior external quantum efficiency, responsivity, and detectivity. *RSC Adv*, 8(69):39579-39592. <https://doi.org/10.1039/c8ra07683a>
- Barsi JA, Lee K, Kvaran G, et al., 2014. The spectral response of the Landsat-8 operational land imager. *Remote Sens*, 6(10): 10232-10251. <https://doi.org/10.3390/rs61010232>
- Bartschi BY, Morse DE, Woolston TL, 1996. The spatial infrared imaging telescope III. *Johns Hopkins APL Tech Dig*, 17(2): 215-225.
- Beil A, Daum R, Harig R, et al., 1998. Remote sensing of atmospheric pollution by passive FTIR spectrometry. *Proc SPIE* 3493, *Spectroscopic Atmospheric Environmental Monitoring Techniques*, p.32-43. <https://doi.org/10.1117/12.332663>
- Bergman TL, Lavine AS, Dewitt DP, et al., 2011. *Introduction to Heat Transfer (6th Ed.)*. John Wiley & Sons, Hoboken, USA.
- Bhan RK, Dhar V, 2019. Recent infrared detector technologies, applications, trends and development of HgCdTe based cooled infrared focal plane arrays and their characterization. *Opto-Electron Rev*, 27(2):174-193. <https://doi.org/10.1016/j.opelre.2019.04.004>
- Blarducci A, Guzzi D, Marcoionni P, et al., 2002. Infrared detection of active fires and burnt areas: theory and observations. *Infrared Phys Technol*, 43(3-5):119-125. [https://doi.org/10.1016/S1350-4495\(02\)00129-9](https://doi.org/10.1016/S1350-4495(02)00129-9)
- Blazejewski ER, Williams GM, McLevige WV, et al., 1994. Advanced LWIR HgCdTe detectors for strategic applications. *Proc SPIE 2217, Aerial Surveillance Sensing Including Obscured and Underground Object Detection*, p.278-290. <https://doi.org/10.1117/12.179946>
- Chang FR, Jiang Z, Wang GW, et al., 2021. Progress of long wavelength infrared focal plane arrays based on antimonide compounds superlattice. *Sci Sin Phys Mech Astron*, 51(2): 027304 (in Chinese). <https://doi.org/10.1360/SSPMA-2020-0307>
- Chatters MEPIV, Eberhardt MB, 2003. *Missile Warning Systems*. Air University Press, Alabama, USA, p.227-234.
- Chauhan D, Perera AGU, Li LH, et al., 2018. Study of infrared photodetectors with wavelength extension mechanism. *Infrared Phys Technol*, 95:148-151. <https://doi.org/10.1016/j.infrared.2018.10.007>
- Chen J, Xi ZL, Qin Q, et al., 2023. Advance in high operating temperature HgCdTe infrared detector. *Infrared Laser Eng*, 52(1):20220462 (in Chinese). <https://doi.org/10.3788/IRLA20220462>
- Chen JS, Shao Y, Guo HD, et al., 2003. Destriping CMODIS data by power filtering. *IEEE Trans Geosci Remote Sens*, 41(9):2119-2124. <https://doi.org/10.1109/TGRS.2003.817206>
- Chen ZC, Tang LB, Hao Q, et al., 2022. Research progress on infrared detection materials and devices of HgCdTe multi-layer heterojunction. *Infrared Technol*, 44(9):889-903 (in Chinese).
- Dehzangi A, Haddadi A, Chevallier R, et al., 2019. Fabrication of 12 μm pixel-pitch 1280 \times 1024 extended short wavelength infrared focal plane array using heterojunction type-II superlattice-based photodetectors. *Semicond Sci Technol*, 34(3):03LT01. <https://doi.org/10.1088/1361-6641/aaf770>
- Ding GZ, Zhang ZY, Guo LW, 2014. Simulation and analysis of workflow and signal-to-noise ratio threshold for SBIRS-GEO early warning satellite's detector. *J Equip Acad*, 25(5):78-82 (in Chinese). <https://doi.org/10.3783/j.issn.2095-3828.2014.05.018>
- Farrah D, Smith KE, Ardila D, et al., 2019. Review: far-infrared instrumentation and technological development for the next decade. *J Astron Telesc Instrum Syst*, 5(2):020901. <https://doi.org/10.1117/1.JATIS.5.2.020901>
- Figier D, Lee J, Corrales E, et al., 2018. HgCdTe detectors grown

- on silicon substrates for observational astronomy. *Proc SPIE* 10709, High Energy, Optical, and Infrared Detectors for Astronomy VIII, Article 1070926. <https://doi.org/10.1117/12.2313401>
- Gao JL, Wen CL, Bao ZJ, et al., 2016. Detecting slowly moving infrared targets using temporal filtering and association strategy. *Front Inform Technol Electron Eng*, 17(11):1176-1185. <https://doi.org/10.1631/FITEE.1601203>
- Gáspár A, Rieke GH, Guillard P, et al., 2021. The quantum efficiency and diffractive image artifacts of Si:As IBC mid-IR detector arrays at 5–10 μm : implications for the JWST/MIRI detectors. *Publ Astron Soc Pac*, 133(1019):014504. <https://doi.org/10.1088/1538-3873/abcd04>
- Ge HN, Xie RZ, Guo JX, et al., 2022. Artificial micro- and nano-structure enhanced long and very long-wavelength infrared detectors. *Acta Phys Sin*, 71(11):110703 (in Chinese). <https://doi.org/10.7498/aps.71.20220380>
- Gendron L, Carras M, Huynh A, et al., 2004. Quantum cascade photodetector. *Appl Phys Lett*, 85(14):2824-2826. <https://doi.org/10.1063/1.1781731>
- Giorgetta FR, Baumann E, Graf M, et al., 2009. Quantum cascade detectors. *IEEE J Quantum Electron*, 45(8):1039-1052. <https://doi.org/10.1109/jqe.2009.2017929>
- Goddijn-Murphy L, Williamson B, 2019. On thermal infrared remote sensing of plastic pollution in natural waters. *Remote Sens*, 11(18):2159. <https://doi.org/10.3390/rs11182159>
- Goldberg AC, 2003. Observation of the launch of the Atlas 5 EELV with a dual-band QWIP focal plane array. *Proc SPIE* 5152, Infrared Spaceborne Remote Sensing XI, p.100-114. <https://doi.org/10.1117/12.504039>
- Gravrand O, Rothman J, Cervera C, et al., 2017. HgCdTe detectors for space and science imaging in France: general issues and latest achievements. *Proc SPIE, Int Conf on Space Optics*, Article 1056240. <https://doi.org/10.1117/12.2296207>
- Grein CH, Young PM, Flatté ME, et al., 1995. Long wavelength InAs/InGaSb infrared detectors: optimization of carrier lifetimes. *J Appl Phys*, 78(12):7143-7152. <https://doi.org/10.1063/1.360422>
- Guilmain BD, 1996. The midcourse space experiment (MSX). *Proc IEEE Aerospace Applications Conf*, p.205-216. <https://doi.org/10.1109/AERO.1996.495885>
- Gunapala SD, Rhiger DR, Jagadish C, 2011. *Advances in Infrared Photodetectors*. Academic Press, Amsterdam, The Netherlands.
- Guo HD, Goodchild MF, Annoni A, 2020. *Manual of Digital Earth*. Springer, Singapore. <https://doi.org/10.1007/978-981-32-9915-3>
- Guo JX, Xie RZ, Wang P, et al., 2022. Infrared photodetectors for multidimensional optical information acquisition. *J Infrared Millim Waves*, 41(1):40-60 (in Chinese). <https://doi.org/10.11972/j.issn.1001-9014.2022.01.002>
- Hair JH, Reuter DC, Tonn SL, et al., 2018. Landsat 9 thermal infrared sensor 2 architecture and design. *Proc IEEE Int Geoscience and Remote Sensing Symp*, p.8841-8844. <https://doi.org/10.1109/IGARSS.2018.8518269>
- Hall DNB, Luppino G, Hodapp KW, et al., 2004. A 4 K \times 4 K HgCdTe astronomical camera enabled by the James Webb Space Telescope NIR detector development program. *Proc SPIE* 5499, Optical and Infrared Detectors for Astronomy, p.1-14. <https://doi.org/10.1117/12.554733>
- Han X, Jiang DW, Wang GW, et al., 2018. Small-pixel long wavelength infrared focal plane arrays based on InAs/GaSb Type-II superlattice. *Infrared Phys Technol*, 89:35-40. <https://doi.org/10.1016/j.infrared.2017.12.004>
- Hao HY, Wu DH, Xu YQ, et al., 2022. Research progress of high performance Sb-based superlattice mid-wave infrared photodetector. *Infrared Laser Eng*, 51(3):20220106 (in Chinese). <https://doi.org/10.3788/IRLA20220106>
- Harland DM, 2021. Infrared Astronomical Satellite. *Encyclopedia Britannica*. <https://www.britannica.com/topic/Infrared-Astronomical-Satellite> [Accessed on Dec. 3, 2021].
- Harwit M, McNutt DP, Shivanandan K, et al., 1966. A liquid nitrogen cooled, rocket borne, infrared telescope. *Appl Opt*, 5(11):1732-1735. <https://doi.org/10.1364/AO.5.001732>
- Hickey M, Boehm N, Foltz R, et al., 2018. Performance of the QWIP focal plane array for NASA's Landsat 9 mission. *SPIE, Berlin, Germany*.
- Hirabayashi M, Narasaki K, Tsunematsu S, et al., 2008. Thermal design and its on-orbit performance of the AKARI cryostat. *Cryogenics*, 48(5-6):189-197. <https://doi.org/10.1016/j.cryogenics.2008.03.003>
- Hoffman AW, Love PJ, Rosbeck JP, 2004. Megapixel detector arrays: visible to 28 μm . *Optical Science and Technology*, p.194-203. <https://doi.org/10.1117/12.516509>
- Höglund L, 2017. T2SL Technology for mid-IR detectors. *Minerva Workshop*, Article 317803.
- Hu WD, Li Q, Chen XS, et al., 2019. Recent progress on advanced infrared photodetectors. *Acta Phys Sin*, 68(12):120701 (in Chinese). <https://doi.org/10.7498/aps.68.20190281>
- Huang M, Chen JX, Xu JJ, et al., 2018. ICP etching for InAs-based InAs/GaAsSb superlattice long wavelength infrared detectors. *Infrared Phys Technol*, 90:110-114. <https://doi.org/10.1016/j.infrared.2018.03.003>
- Hudson JR, 1969. *Infrared System Engineering*. John Wiley & Sons, New York, USA.
- Ishihara D, Wada T, Watarai H, et al., 2003. Evaluation of the mid- and near-infrared focal plane arrays for Japanese infrared astronomical satellite ASTRO-F. *Proc SPIE* 4850, IR Space Telescopes and Instruments, p.1008-1019. <https://doi.org/10.1117/12.461225>
- Ivanov R, Höglund L, Ramos D, et al., 2019. T2SL development for space at IRnova: from eSWIR to VLWIR. *Proc SPIE* 11151, Sensors, Systems, and Next-Generation Satellites XXIII, Article 1115111. <https://doi.org/10.1117/12.2533247>
- James WB, 2019. High performance infrared for extreme precision radial velocity measurement detectors. *Extreme Precision for Radial Velocity IV*, Grindelwald, Switzerland.
- Jhabvala M, Choi KK, Gunapala S, et al., 2020. QWIPs, SLS, Landsat and the International Space Station. *Proc SPIE* 11288, Quantum Sensing and Nano Electronics and Photonics XVII, Article 1128802. <https://doi.org/10.1117/12.2539147>
- Jiang ZH, Wu YN, Lu Z, et al., 2021. On-orbit performance of the FY-4 GIIRS stirling cryocooler over 2 years. *J Low Temp Phys*, 203(1-2):244-253. <https://doi.org/10.1007/s10909-021-02570-2>

- Joshi A, Kataria N, Garnett J, et al., 2021. A low SWAP-C 10-micron pitch 3-megapixel full motion video MWIR imaging system. *Proc SPIE 11741, Infrared Technology and Applications XLVII, Article 117411M*.
<https://doi.org/10.1117/12.2588209>
- Karim A, Andersson JY, 2013. Infrared detectors: advances, challenges and new technologies. *IOP Conf Ser Mater Sci Eng*, 51:012001.
<https://doi.org/10.1088/1757-899X/51/1/012001>
- Karthikeyan L, Chawla I, Mishra AK, 2020. A review of remote sensing applications in agriculture for food security: crop growth and yield, irrigation, and crop losses. *J Hydrol*, 586:124905. <https://doi.org/10.1016/j.jhydrol.2020.124905>
- Keller LD, Herter TL, Stacey GJ, et al., 2000. FORCAST: a facility 5- to 40- μm camera for SOFIA. *Proc SPIE 4014, Airborne Telescope Systems*, p.86-97.
<https://doi.org/10.1117/12.389130>
- Kessler MF, 1989. The Infrared Space Observatory (ISO) and its instruments. *Proc SPIE 1130, New Technologies for Astronomy*, p.194-201. <https://doi.org/10.1117/12.961523>
- Kessler MF, 1993. Infrared Space Observatory: mission and spacecraft. *Proc SPIE 2019, Infrared Spaceborne Remote Sensing*, p.9-14. <https://doi.org/10.1117/12.157824>
- Khanal S, Fulton J, Shearer S, 2017. An overview of current and potential applications of thermal remote sensing in precision agriculture. *Comput Electron Agric*, 139:22-32.
<https://doi.org/10.1016/j.compag.2017.05.001>
- Kimukin I, Biyikli N, Kartaloglu T, et al., 2004. High-speed InSb photodetectors on GaAs for mid-IR applications. *IEEE J Select Top Quantum Electron*, 10(4):766-770.
<https://doi.org/10.1109/jstqe.2004.833891>
- Kinch MA, 2000. Fundamental physics of infrared detector materials. *J Electron Mater*, 29(6):809-817.
<https://doi.org/10.1007/s11664-000-0229-7>
- King DF, Radford WA, Patten EA, et al., 2006. Third-generation 1280 \times 720 FPA development status atraytheon vision systems. *Proc SPIE 6206, Infrared Technology and Applications XXXII, Article 62060W*.
<https://doi.org/10.1117/12.673241>
- Kopytko M, Rogalski A, 2022. New insights into the ultimate performance of HgCdTe photodiodes. *Sens Actuat A Phys*, 339:113511. <https://doi.org/10.1016/j.sna.2022.113511>
- Kruse PW, 2001. Uncooled Thermal Imaging: Arrays, Systems, and Applications. SPIE, Bellingham, USA.
<https://doi.org/10.1117/3.415351>
- Lao YF, Perera AGU, Li LH, et al., 2014. Tunable hot-carrier photodetection beyond the bandgap spectral limit. *Nat Photon*, 8(5):412-418.
<https://doi.org/10.1038/nphoton.2014.80>
- Laureijs R, Racca G, Stagnaro L, et al., 2014. Euclid mission status. *Proc SPIE 9143, Space Telescopes and Instrumentation 2014: Optical, Infrared, and Millimeter Wave*, p.132-139.
<https://doi.org/10.1117/12.2054883>
- Lewis GN, Postol TA, 1997. Future challenges to ballistic missile defense. *IEEE Spectr*, 34(9):60-68.
<https://doi.org/10.1109/6.619381>
- Li JD, 2021. Satellite Remote Sensing Technologies. Springer, Beijing, China.
- Li JD, Qiao K, Yang D, 2021. Design and Definition of On-orbit Imaging Quality of High-Resolution Optical Remote Sensing Satellites. National Defense Industry Press, Beijing, China (in Chinese).
- Li LM, He L, Wu X, et al., 2021. Wideband cryogenic amplifier for a superconducting nanowire single-photon detector. *Front Inform Technol Electron Eng*, 22(12):1666-1676.
<https://doi.org/10.1631/FITEE.2100525>
- Lin CHT, Anselm KA, Kuo CH, et al., 2000. Type-II InAs/InGaSb SL photodetectors. *Proc SPIE 3948, Photodetectors: Materials and Devices V*, p.133-144.
<https://doi.org/10.1117/12.382112>
- Liu JK, Xiao L, Liu Y, et al., 2019. Development of long-wavelength infrared detector and its space-based application requirements. *Chin Phys B*, 28(2):028504.
<https://doi.org/10.1088/1674-1056/28/2/028504>
- Liu YN, Sun DX, Hu XN, et al., 2019. The advanced hyperspectral imager: aboard China's GaoFen-5 satellite. *IEEE Geosci Remote Sens Mag*, 7(4):23-32.
<https://doi.org/10.1109/MGRS.2019.2927687>
- Lockwood R, Cooley T, Nadile R, et al., 2006. Advanced responsive tactically-effective military imaging spectrometer (ARTEMIS) design. *Proc IEEE Int Symp on Geoscience and Remote Sensing*, p.1628-1630.
<https://doi.org/10.1109/IGARSS.2006.420>
- Long D, 1977. Photovoltaic and photoconductive infrared detectors. In: Keyes RJ (Ed.), *Optical and Infrared Detectors*. Springer Berlin Heidelberg, Germany, p.101-147.
https://doi.org/10.1007/3540101764_12
- Long MS, Wang P, Fang HH, et al., 2019. Progress, challenges, and opportunities for 2D material based photodetectors. *Adv Funct Mater*, 29(19):1803807.
<https://doi.org/10.1002/adfm.201803807>
- Lv Q, Dou Y, Niu X, et al., 2015. Classification of Tiangong-1 hyperspectral remote sensing image via contextual sparse coding. *Proc Int Conf on Machine Learning and Cybernetics*, p.128-133.
<https://doi.org/10.1109/ICMLC.2015.7340910>
- Lyu WD, Deng XG, Wang QW, et al., 2022. Infrared detector butted technology for space. *Infrared Technol*, 44(10):999-1008 (in Chinese).
- Ma XZ, Tang LB, Zhang YP, et al., 2023. Research progress of silicon-based BIB infrared detector. *Infrared Technol*, 45(1):1-14 (in Chinese).
- Manurkar P, Ramezani-Darvish S, Nguyen BM, et al., 2010. High performance long wavelength infrared mega-pixel focal plane array based on type-II superlattices. *Appl Phys Lett*, 97(19):193505.
<https://doi.org/10.1063/1.3514244>
- Martyniuk P, Antoszewski J, Martyniuk M, et al., 2014. New concepts in infrared photodetector designs. *Appl Phys Rev*, 1(4):041102. <https://doi.org/10.1063/1.4896193>
- Migdall A, Polyakov S, Fan JY, et al., 2013. Single-Photon Generation and Detection. Elsevier, Amsterdam, The Netherlands.
- Mill JD, O'Neil RR, Price S, et al., 1994. Midcourse space experiment: introduction to the spacecraft, instruments, and scientific objectives. *J Spacecr Rock*, 31(5):900-907.
<https://doi.org/10.2514/3.55673>
- Miller JL, 1994. Principles of Infrared Technology: a Practical

- Guide to the State of the Art. Springer, New York, USA. <https://doi.org/10.1007/978-1-4615-7664-8>
- Miller JL, 2004. *Photonics Rules of Thumb: Optics, Electro-Optics, Fiber Optics, and Lasers* (2nd Ed.). McGraw-Hill, New York, USA.
- Montanaro M, McCorkel J, Tveekrem J, et al., 2018. Landsat 9 thermal infrared sensor 2 preliminary stray light assessment. *Proc IEEE Int Geoscience and Remote Sensing Symp*, p.8853-8856. <https://doi.org/10.1109/IGARSS.2018.8519394>
- Nakagawa T, Matsuhara H, Kawakatsu Y, 2012. The next-generation infrared space telescope SPICA. *Proc SPIE 8442, Space Telescopes and Instrumentation: Optical, Infrared, and Millimeter Wave*, Article 84420O. <https://doi.org/10.1117/12.927243>
- Ni GQ, Hao QW, Zhang HL, et al., 2006. Applications of multi-color FPA from the DSP and SBIRS space early warning systems. *Laser Infrared*, 36(11):1016-1019 (in Chinese). <https://doi.org/10.3969/j.issn.1001-5078.2006.11.003>
- Onaka T, Matsuhara H, Wada T, et al., 2010. AKARI warm mission. *Proc SPIE 7731, Space Telescopes and Instrumentation: Optical, Infrared, and Millimeter Wave*, Article 77310M. <https://doi.org/10.1117/12.856568>
- Pan XK, Jiang MJ, Wang D, et al., 2023. Application and frontier trend of infrared-terahertz photoelectric detector. *Chin J Quantum Electron*, 40(2):217-237 (in Chinese). <https://doi.org/10.3969/j.issn.1007-5461.2023.02.005>
- Park H, Choi J, 2021. Mineral detection using sharpened VNIR and SWIR bands of Worldview-3 satellite imagery. *Sustainability*, 13(10):5518. <https://doi.org/10.3390/su13105518>
- Park S, Feinberg LD, Homan JL, et al., 2019. JWST overview and successful operation of the cryo-vac test at NASA JSC during hurricane harvey. *Proc IEEE Aerospace Conf*, p.1-11. <https://doi.org/10.1109/AERO.2019.8741592>
- Paschotta R, 2008. *Encyclopedia of Laser Physics and Technology*. Wiley, Weinheim, Germany.
- Paxton LJ, Meng CI, Anderson DE, et al., 1996. MSX—a multi-use space experiment. *Johns Hopkins APL Tech Dig*, 17(1): 19-34.
- Perera AGU, Chauhan D, Lao YF, et al., 2016. Infrared photo-detector with wavelength extension beyond the spectral limit. *Proc SPIE 9844, Automatic Target Recognition XXVI*, Article 98440X. <https://doi.org/10.1117/12.225264>
- Pérez-Cabello F, Montorio R, Alves DB, 2021. Remote sensing techniques to assess post-fire vegetation recovery. *Curr Opin Environ Sci Health*, 21:100251. <https://doi.org/10.1016/j.coesh.2021.100251>
- Piotrowski J, Gawron W, 1997. Ultimate performance of infrared photodetectors and figure of merit of detector material. *Infrared Phys Technol*, 38(2):63-68. [https://doi.org/10.1016/S1350-4495\(96\)00030-8](https://doi.org/10.1016/S1350-4495(96)00030-8)
- Pipher JL, McMurtry CW, Cabrera MS, et al., 2021. Mid-infrared detector array technologies for SOFIA and sub-orbital observatory instruments. *J Astron Instrum*, 10(2):2150008. <https://doi.org/10.1142/S2251171721500082>
- Price SD, Tedesco EF, Cohen M, et al., 1998. Astronomy on the midcourse space experiment. *Symp-Int Astron Union*, 179:115-117. <https://doi.org/10.1017/S0074180900128347>
- Qin G, Ji FQ, Xia LK, et al., 2021. HgCdTe high operation temperature infrared detectors. *Infrared Laser Eng*, 50(4): 20200328. <https://doi.org/10.3788/IRLA20200328>
- Ranganath BK, Pradeep N, Manjula VB, et al., 2004. Detection of diseased rubber plantations using satellite remote sensing. *J Ind Soc Remote Sens*, 32(1):49-58. <https://doi.org/10.1007/BF03030847>
- Reibel Y, Pere-Laperne N, Augey T, et al., 2014. Getting small: new 10 μ m pixel pitch cooled infrared products. *Proc SPIE 9070, Infrared Technology and Applications XL*, Article 907034. <https://doi.org/10.1117/12.2051654>
- Ressler ME, Cho H, Lee RAM, et al., 2008. Performance of the JWST/MIRI Si:As detectors. *Proc SPIE 7021, High Energy, Optical, and Infrared Detectors for Astronomy III*, p.756-759. <https://doi.org/10.1117/12.789606>
- Ressler ME, Sukhatme KG, Franklin BR, et al., 2015. The mid-infrared instrument for the *James Webb Space Telescope*, VIII: the MIRI focal plane system. *Publ Astron Soc Pac*, 127(953):675-685. <https://doi.org/10.1086/682258>
- Reuter DC, Richardson CM, Pellerano FA, et al., 2015. The thermal infrared sensor (TIRS) on Landsat 8: design overview and pre-launch characterization. *Remote Sens*, 7(1): 1135-1153. <https://doi.org/10.3390/rs70101135>
- Rieke GH, 2007. Infrared detector arrays for astronomy. *Ann Rev Astron Astrophys*, 45:77-115. <https://doi.org/10.1146/annurev.astro.44.051905.092436>
- Rieke GH, Wright GS, Böker T, et al., 2015. The mid-infrared instrument for the *James Webb Space Telescope*, I: introduction. *Publ Astron Soc Pac*, 127(953):584-594. <https://doi.org/10.1086/682252>
- Robbins RC, 2019. The interagency challenges of hypersonic strike weapons. *InterAgency J*, 10(2):17-29.
- Roberts T, Roush F, 2007. Cryogenic refrigeration systems as an enabling technology in space sensing missions. *Int Cryo-cooler Conf*, p.595-604.
- Rodriguez JI, 2017. Feasibility of passive cryogenic cooling for solar powered outer planetary missions. *Proc 47th Int Conf on Environmental Systems*, p.1-19.
- Roelfsema PR, Shibai H, Armus L, et al., 2018. SPICA—a large cryogenic infrared space telescope: unveiling the obscured universe. *Publ Astron Soc Aust*, 35:e030. <https://doi.org/10.1017/pasa.2018.15>
- Roellig TL, McMurtry CW, Greene TP, et al., 2020. Mid-infrared detector development for the Origins Space Telescope. *J Astron Telesc Instrum Syst*, 6(4):041503. <https://doi.org/10.1117/1.JATIS.6.4.041503>
- Rogalski A, 2002. Infrared detectors: an overview. *Infrared Phys Technol*, 43(3-5):187-210. [https://doi.org/10.1016/S1350-4495\(02\)00140-8](https://doi.org/10.1016/S1350-4495(02)00140-8)
- Rogalski A, 2003a. Infrared detectors: status and trends. *Prog Quantum Electron*, 27(2-3):59-210. [https://doi.org/10.1016/S0079-6727\(02\)00024-1](https://doi.org/10.1016/S0079-6727(02)00024-1)
- Rogalski A, 2003b. Quantum well photoconductors in infrared detector technology. *J Appl Phys*, 93(8):4355-4391. <https://doi.org/10.1063/1.1558224>
- Rogalski A, 2005. HgCdTe infrared detector material: history, status and outlook. *Rep Prog Phys*, 68(10):2267-2336. <https://doi.org/10.1088/0034-4885/68/10/R01>
- Rogalski A, 2008. New material systems for third generation

- infrared photodetectors. *Opto-Electron Rev*, 16(4):458-482. <https://doi.org/10.2478/s11772-008-0047-7>
- Rogalski A, 2009. Infrared detectors for the future. *Acta Phys Pol A*, 116(3):389-406. <https://doi.org/10.12693/APhysPolA.116.389>
- Rogalski A, 2010. Infrared Detectors (2nd Ed.). CRC Press, Boca Raton, USA. <https://doi.org/10.1201/b10319>
- Rogalski A, 2011. Recent progress in infrared detector technologies. *Infrared Phys Technol*, 54(3):136-154. <https://doi.org/10.1016/j.infrared.2010.12.003>
- Rogalski A, 2012. History of infrared detectors. *Opto-Electron Rev*, 20(3):279-308. <https://doi.org/10.2478/s11772-012-0037-7>
- Rogalski A, 2017. Next decade in infrared detectors. Proc 10433, Electro-Optical and Infrared Systems: Technology and Applications XIV, Article 104330L. <https://doi.org/10.1117/12.2300779>
- Rogalski A, 2019. Infrared and Terahertz Detectors (3rd Ed.). CRC Press, Boca Raton, USA. <https://doi.org/10.1201/b21951>
- Rogalski A, Antoszewski J, Faraone L, 2009. Third-generation infrared photodetector arrays. *J Appl Phys*, 105(9):091101. <https://doi.org/10.1063/1.3099572>
- Rogalski A, Martyniuk P, Kopytko M, 2016. Challenges of small-pixel infrared detectors: a review. *Rep Prog Phys*, 79(4):046501. <https://doi.org/10.1088/0034-4885/79/4/046501>
- Rogalski A, Martyniuk P, Kopytko M, 2017. InAs/GaSb type-II superlattice infrared detectors: future prospect. *Appl Phys Rev*, 4(3):031304. <https://doi.org/10.1063/1.4999077>
- Rogalski A, Kopytko M, Martyniuk P, 2019a. Two-dimensional infrared and terahertz detectors: outlook and status. *Appl Phys Rev*, 6(2):021316. <https://doi.org/10.1063/1.5088578>
- Rogalski A, Martyniuk P, Kopytko M, 2019b. Type-II superlattice photodetectors versus HgCdTe photodiodes. *Prog Quantum Electron*, 68:100228. <https://doi.org/10.1016/j.pquantelec.2019.100228>
- Rogalski A, Martyniuk P, Kopytko M, et al., 2020. InAsSb-based infrared photodetectors: thirty years later on. *Sensors*, 20(24):7047. <https://doi.org/10.3390/s20247047>
- Sanders DB, 2004. The cosmic evolution of luminous infrared galaxies: from IRAS to ISO, SCUBA and SIRTf. *Adv Space Res*, 34(3):535-542. <https://doi.org/10.1016/j.asr.2003.04.037>
- Saraf AK, Rawat V, Banerjee P, et al., 2008. Satellite detection of earthquake thermal infrared precursors in Iran. *Nat Hazards*, 47(1):119-135. <https://doi.org/10.1007/s11069-007-9201-7>
- Schneider H, Liu HC, 2007. Quantum Well Infrared Photodetectors: Physics and Applications. Springer Berlin Heidelberg, Germany. <https://doi.org/10.1007/978-3-540-36324-8>
- Schwalm M, Barry M, Perron G, et al., 2005. Cryogenic telescope, scanner, and imaging optics for the wide-field infrared survey explorer (WISE). Proc SPIE 5904, Cryogenic Optical Systems and Instruments XI, Article 59040K. <https://doi.org/10.1117/12.617653>
- Sclar N, 1984. Properties of doped silicon and germanium infrared detectors. *Prog Quantum Electron*, 9(3):149-257. [https://doi.org/10.1016/0079-6727\(84\)90001-6](https://doi.org/10.1016/0079-6727(84)90001-6)
- Seenipandi K, Ramachandran KK, Ghadei P, et al., 2021. Seasonal variability of sea surface temperature in Southern Indian coastal water using Landsat 8 OLI/TIRS images. In: Rani M, Seenipandi K, Rehman S, et al. (Eds.), Remote Sensing of Ocean and Coastal Environments. Elsevier, Amsterdam, The Netherlands, p.277-295. <https://doi.org/10.1016/B978-0-12-819604-5.00016-0>
- Sessler AM, Cornwall JM, Dietz B, et al., 2020. Countermeasures: a Technical Evaluation of the Operational Effectiveness of the Planned US National Missile Defense System. Union of Concerned Scientists and MIT Security Studies Program, Cambridge, MA, USA.
- Shang LT, Wang J, Xing WR, et al., 2021. Advances in type-II superlattice infrared detector technology at home and abroad. *Laser Infrared*, 51(6):683-694 (in Chinese). <https://doi.org/10.3969/j.issn.1001-5078.2021.06.001>
- Shen MZ, Lin XD, Ma WL, et al., 1996. Cryogenic test of an all-aluminum infrared optical system. Proc SPIE 2814, Cryogenic Optical Systems and Instruments VII, p.121-125. <https://doi.org/10.1117/12.254154>
- Shi Q, Zhang SK, Wang JL, et al., 2022. Progress on nBn infrared detectors. *J Infrared Millim Waves*, 41(1):139-150. <https://doi.org/10.11972/j.issn.1001-9014.2022.01.010>
- Shi WH, Lv WM, Sun TY, et al., 2019. Optoelectronic platform and technology. *Front Inform Technol Electron Eng*, 20(4):439-457. <https://doi.org/10.1631/FITEE.1800451>
- Shinozaki K, Sato Y, Tokoku C, et al., 2020. Mechanical cooler system for the infrared space mission SPICA. Proc SPIE 11443, Space Telescopes and Instrumentation: Optical, Infrared, and Millimeter Wave, Article 1144329. <https://doi.org/10.1117/12.2562175>
- Singer C, Massoni JA, Mossbacher B, et al., 1991. Infrared Space Observatory optical subsystem. Proc SPIE 1494, Space Astronomical Telescopes and Instruments, p.255-264. <https://doi.org/10.1117/12.46729>
- Singh V, Sharma N, Singh S, 2020. A review of imaging techniques for plant disease detection. *Artif Intell Agric*, 4:229-242. <https://doi.org/10.1016/j.aiia.2020.10.002>
- Smith MS, 2006. Military Space Programs: Issues Concerning DOD's SBIRS and STSS Programs. Order Code RS21148, Congressional Research Service, Washington, USA.
- Sobrinho JA, del Frate F, Drusch M, et al., 2016. Review of thermal infrared applications and requirements for future high-resolution sensors. *IEEE Trans Geosci Remote Sens*, 54(5):2963-2972. <https://doi.org/10.1109/TGRS.2015.2509179>
- Song SF, Huang LY, Tian Z, 2022. The theory and research advancement of HgCdTe detectors at high operating temperature. *Laser Infrared*, 52(5):636-640 (in Chinese). <https://doi.org/10.3969/j.issn.1001-5078.2022.05.002>
- Stair AT, 1996. MSX design parameters driven by targets and backgrounds. *Johns Hopkins APL Tech Dig*, 17(1):11-18.
- Starr B, Mears L, Fulk C, et al., 2016. RVS large format arrays for astronomy. Proc SPIE 9915, High Energy, Optical, and Infrared Detectors for Astronomy VII, Article 99152X. <https://doi.org/10.1117/12.2233033>
- Sweeney SJ, Eales TD, Marko IP, 2020. The physics of mid-infrared semiconductor materials and heterostructures. In: Tourmié E, Cerutti L (Eds.), Mid-infrared Optoelectronics. Elsevier, Duxford, UK, p.3-56.

- <https://doi.org/10.1016/B978-0-08-102709-7.00001-2>
- Swindells I, Wheeler R, Jerram P, et al., 2023. Infrared detector developments at Teledyne e2v for current and future missions. Proc SPIE 12777, Int Conf on Space Optics, Article 1277760. <https://doi.org/10.1117/12.2691107>
- Szapkowski DM, Jensen JLR, 2019. A review of the applications of remote sensing in fire ecology. *Remote Sens*, 11(22): 2638. <https://doi.org/10.3390/rs11222638>
- Tan CL, Mohseni H, 2018. Emerging technologies for high performance infrared detectors. *Nanophotonics*, 7(1):169-197. <https://doi.org/10.1515/nanoph-2017-0061>
- Teng Y, Zhao Y, Wu QH, et al., 2019. High-performance long-wavelength InAs/GaSb superlattice detectors grown by MOCVD. *IEEE Photon Technol Lett*, 31(2):185-188. <https://doi.org/10.1109/LPT.2018.2889575>
- Tidrow MZ, Dyer WR, 2001. Infrared sensors for ballistic missile defense. *Infrared Phys Technol*, 42(3-5):333-336. [https://doi.org/10.1016/S1350-4495\(01\)00092-5](https://doi.org/10.1016/S1350-4495(01)00092-5)
- Ting DZ, Soibel A, Khoshakhlagh A, et al., 2023. InAs/InAsSb superlattice infrared detectors. *Opto-Electron Rev*, 31: e144565.
- Watson J, Zondervan K, 2008. The Missile Defense Agency's space tracking and surveillance system. Proc SPIE 7106, Sensors, Systems, and Next-Generation Satellites XII, Article 710617. <https://doi.org/10.1117/12.801937>
- Weeks SJ, Currie B, Bakun A, 2002. Massive emissions of toxic gas in the Atlantic. *Nature*, 415(6871):493-494. <https://doi.org/10.1038/415493b>
- Wei YJ, Gin A, Razeghi M, et al., 2002. Type II InAs/GaSb superlattice photovoltaic detectors with cutoff wavelength approaching 32 μm . *Appl Phys Lett*, 81(19):3675-3677. <https://doi.org/10.1063/1.1520699>
- Wiedner MC, Aalto S, Armus L, et al., 2021. Origins space telescope: from first light to life. *Exp Astron*, 51(3):595-624. <https://doi.org/10.1007/s10686-021-09782-0>
- Wójtowicz M, Wójtowicz A, Piekarczyk J, 2016. Application of remote sensing methods in agriculture. *Commun Biometry Crop Sci*, 11(1):31-50.
- Wright GS, Wright D, Goodson GB, et al., 2015. The mid-infrared instrument for the *James Webb Space Telescope*, II: design and build. *Publ Astron Soc Pac*, 127(953):595-611. <https://doi.org/10.1086/682253>
- Wu BH, Xia GQ, Li ZH, et al., 2002. Sulphur passivation of the InGaAsSb/GaSb photodiodes. *Appl Phys Lett*, 80(7): 1303-1305. <https://doi.org/10.1063/1.1448383>
- Wu YN, Dong DP, Lu Y, 2019. Spaceborne Cryocooler Technology. Science Press, Beijing, China (in Chinese).
- Yang CH, 2020. Remote sensing and precision agriculture technologies for crop disease detection and management with a practical application example. *Engineering*, 6(5):528-532. <https://doi.org/10.1016/j.eng.2019.10.015>
- Yang RQ, Tian ZB, Klem JF, et al., 2010. Interband cascade photovoltaic devices. *Appl Phys Lett*, 96(6):063504. <https://doi.org/10.1063/1.3313934>
- Ye ZH, Li HH, Wang JD, et al., 2022. Recent hotspots and innovative trends of infrared photon detectors. *J Infrared Millim Waves*, 41(1):15-39 (in Chinese). <https://doi.org/10.11972/j.issn.1001-9014.2022.01.001>
- Yin LM, Liu YQ, Li HW, 2013. Cold optics technology to achieve high-accuracy infrared detection. *Infrared Technol*, 35(9):535-540 (in Chinese).
- Young E, 2002. Detector Needs for Long Wavelength Astrophysics. Report of the Working Group to NASA.
- Zhang J, Lu Y, Huang H, et al., 2021. Review of the overall parameter analysis of detection system of STSS. Proc SPIE 11763, 7th Symp on Novel Photoelectronic Detection Technology and Applications, Article 1176395. <https://doi.org/10.1117/12.2587650>
- Zhang KJ, 2021. Research progress and trends of high operating temperature infrared detectors. *Infrared Technol*, 43(8): 766-772 (in Chinese).
- Zhang S, Hu Y, Hao Q, 2020. Advances of sensitive infrared detectors with HgTe colloidal quantum dots. *Coatings*, 10(8): 760. <https://doi.org/10.3390/coatings10080760>
- Zhang X, Guo YZ, Wan XM, et al., 2010. Simulation of early warning and detection capability of ballistic missile in boosting phase based on infrared characteristic. *Shipboard Electron Countermeas*, 33(5):92-95 (in Chinese). <https://doi.org/10.16426/j.cnki.jcdzdk.2010.05.006>
- Zhao W, Wang X, Liu H, et al., 2020. Development of space-based diffractive telescopes. *Front Inform Technol Electron Eng*, 21(6):884-902. <https://doi.org/10.1631/FITEE.1900529>
- Zhao X, Xiao ZQ, Kang Q, et al., 2010. Overview of the Fourier transform hyperspectral imager (HSI) boarded on HJ-1A satellite. Proc IEEE Int Geoscience and Remote Sensing Symp, p.4272-4274. <https://doi.org/10.1109/IGARSS.2010.5649250>
- Zheng L, Tidrow MZ, Novello A, et al., 2008. Type II strained layer superlattice: a potential infrared sensor material for space. Proc SPIE 6900, Quantum Sensing and Nanophotonic Devices V, Article 69000F. <https://doi.org/10.1117/12.768420>
- Zheng L, Tidrow M, Aitchison L, et al., 2010. Developing high-performance III-V superlattice IRFPAs for defense: challenges and solutions. Proc SPIE 7660, Infrared Technology and Applications XXXVI, Article 76601E. <https://doi.org/10.1117/12.852239>
- Zhu P, Xiao L, Sun T, et al., 2022. Research progress of micro-nano structures enhanced infrared detectors. *Infrared Laser Eng*, 51(1):20210826 (in Chinese). <https://doi.org/10.3788/IRLA20210826>